



Defense Threat Reduction Agency  
8725 John J. Kingman Road, MS  
6201 Fort Belvoir, VA 22060-6201



DTRA-TR-12-46

# TECHNICAL REPORT

## Next Generation Structural Composite Using Surface Grown Carbon Nanotubes

Approved for public release, distribution is unlimited.

October 2012

HDTRA1-08-1-0017

Mahmoud Reda Taha, PhD

Prepared by:  
Regents of the Univ. of Mexico  
MSC01 1247  
1700 Lomas Blvd, NE, Ste.  
2200  
Albuquerque, NM 87131-0001

**DESTRUCTION NOTICE:**

Destroy this report when it is no longer needed.  
Do not return to sender.

PLEASE NOTIFY THE DEFENSE THREAT REDUCTION  
AGENCY, ATTN: DTRIAC/ J-3 ONIUI , 8725 JOHN J. KINGMAN ROAD,  
MS-6201, FT BELVOIR, VA 22060-6201, IF YOUR ADDRESS  
IS INCORRECT, IF YOU WISH THAT IT BE DELETED FROM THE  
DISTRIBUTION LIST, OR IF THE ADDRESSEE IS NO  
LONGER EMPLOYED BY YOUR ORGANIZATION.

<b>REPORT DOCUMENTATION PAGE</b>			<i>Form Approved</i> <i>OMB No. 0704-0188</i>	
Public reporting burden for this collection of information is estimated to average 1 hour per response, including the time for reviewing instructions, searching existing data sources, gathering and maintaining the data needed, and completing and reviewing this collection of information. Send comments regarding this burden estimate or any other aspect of this collection of information, including suggestions for reducing this burden to Department of Defense, Washington Headquarters Services, Directorate for Information Operations and Reports (0704-0188), 1215 Jefferson Davis Highway, Suite 1204, Arlington, VA 22202-4302. Respondents should be aware that notwithstanding any other provision of law, no person shall be subject to any penalty for failing to comply with a collection of information if it does not display a currently valid OMB control number. <b>PLEASE DO NOT RETURN YOUR FORM TO THE ABOVE ADDRESS.</b>				
<b>1. REPORT DATE (DD-MM-YYYY)</b> 00-10-2012		<b>2. REPORT TYPE</b> Final Report		<b>3. DATES COVERED (From - To)</b> March 2008 - March 2012
<b>4. TITLE AND SUBTITLE</b> Next Generation Structural Composites Using Surface Grown Carbon Nanotubes			<b>5a. CONTRACT NUMBER</b> N/A	
			<b>5b. GRANT NUMBER</b> HDTRA1-08-1-0017	
			<b>5c. PROGRAM ELEMENT NUMBER</b> N/A	
<b>6. AUTHOR(S)</b> Taha, Mahmoud Reda, PhD, PEng (PI)			<b>5d. PROJECT NUMBER</b> N/A	
			<b>5e. TASK NUMBER</b> N/A	
			<b>5f. WORK UNIT NUMBER</b> N/A	
<b>7. PERFORMING ORGANIZATION NAME(S) AND ADDRESS(ES)</b> Regents of the University of New Mexico Div. of Sponsored Project Services, MSC01 1247 1700 Lomas Blvd, NE, Ste. 2200 Albuquerque, NM 87131-0001			<b>8. PERFORMING ORGANIZATION REPORT NUMBER</b>  N/A	
<b>9. SPONSORING / MONITORING AGENCY NAME(S) AND ADDRESS(ES)</b> DTRA/BE-BCR J9/BAS J. Reed 8725 John J. Kingman Road MSC 6201 Fort Belvoir, VA 22060-6201			<b>10. SPONSOR/MONITOR'S ACRONYM(S)</b>  DTRA	
			<b>11. SPONSOR/MONITOR'S REPORT NUMBER(S)</b> DTRA-TR-12-46	
<b>12. DISTRIBUTION / AVAILABILITY STATEMENT</b> Approved for public release; distribution is unlimited.				
<b>13. SUPPLEMENTARY NOTES</b>  N/A				
<b>14. ABSTRACT</b> The goal of the project was to develop the next generation of structural composites with enhanced impact-resistance capabilities over the current technology using carbon nanotubes (CNTs) and to understand the basic science behind this development. Our objectives included 1- Investigating methods to grow CNTs on the surface of carbon fabrics 2- Investigating methods to uniformly disperse CNTs in carbon fabrics 3- Investigating methods to fabricate carbon fabrics using CNTs 4- Mechanical characterization of the new composite including its impact strength 5- Understand the basic science behind its improved mechanical performance and impact strength All the above objectives have been accomplished. Six graduate students performed their graduate degrees during the project period. The research results have been published in 3 pending patents, 6 conference papers and 16 scholarly journal papers.				
<b>15. SUBJECT TERMS</b> Carbon nanotubes, nanocomposites, impact resistance, mechanical characterization				
<b>16. SECURITY CLASSIFICATION OF:</b> U			<b>17. LIMITATION OF ABSTRACT</b>  UU	<b>18. NUMBER OF PAGES</b>  34
<b>a. REPORT</b> U	<b>b. ABSTRACT</b> U	<b>c. THIS PAGE</b> U		
			<b>19b. TELEPHONE NUMBER (include area code)</b> (505) 277-1258	

## TABLE OF CONTENTS

1. Cover Sheet .....	i
2. Major Goals .....	2
3. Accomplishments .....	2
3.1. Materials Properties .....	2
3.2. CNTs-Epoxy Nanocomposite Fabrication.....	3
3.3. Fabrication of the CFRP Composite .....	4
3.4. On and off-axis tension tests .....	5
3.5. Flexure test .....	11
3.6. Thermal stability .....	12
3.7. Microstructural investigation .....	14
3.8. Lap shear splice characterization.....	15
3.9. Fracture Toughness Testing.....	18
3.10. Impact Testing .....	22
4. Summary of Accomplishments.....	27
5. Personnel supported .....	28
6. Scholarly Journal Publications .....	29
7. Papers in Conference Proceedings and Public Presentations .....	29
8. New discoveries, inventions, or patent disclosures .....	30
9. Honors/Awards.....	30
10. Quad chart.....	30

## TABLE OF FIGURES

Figure 1. Schematic representation of CNTs mechanism .....	2
Figure 2. Functionalization of CNTs .....	4
Figure 3. Fabrication of carbon fiber fabric .....	4
Figure 4. Tension test of CFRP composite .....	5
Figure 5. Failure mechanism for on and off-axis CFRP coupons.....	6
Figure 6. Stress-strain relationships for CFRP off-axis composite coupons for various chemical treatments .....	7
Figure 7. Stress-strain relationships for CFRP off-axis composite coupons with various MWCNTs-contents.....	9
Figure 8. Stress-strain relationships for CFRP on-axis composite coupons with various MWCNTs-contents .....	10
Figure 9. Normalized tensile toughness for CFRP composites coupons with various MWCNTs-contents .....	11
Figure 10. Bending stress-strain relationships for various MWCNTs-epoxy nanocomposites .....	12
Figure 11. DSC results for various MWCNTs-epoxy nanocomposites .....	13
Figure 12. TGA results for various MWCNTs-epoxy nanocomposites .....	14
Figure 13. SEM images for CNT-epoxy nano-composites with various CNTs surface conditions.....	15
Figure 14. Double lap joint configurations .....	16
Figure 15. Double lap joint test setup .....	16
Figure 16. Shear stress-strain of FRP lap splice with various MWCNTs loadings .....	17
Figure 17. Comparison of shear strength and failure strain for different MWCNTs epoxy nanocomposites .....	18
Figure 18. DCB test set-up for Interlaminar fracture toughness testing .....	19
Figure 19. Crack propagation for the 0.5% COOH-MWCNT/epoxy FRP composites .....	20
Figure 20. Resistance curve (R-curve) for MWCNT/epoxy FRP composites .....	21
Figure 21. Schematic for delamination growth mechanism .....	21
Figure 22. Comparison for the critical energy release rate corresponding to 6 mm delamination .....	22
Figure 23. CEAST® 9350 impact tester.....	23
Figure 24. Velocity-time response for various COOH-MWCNTs composite plates .....	24
Figure 25. Energy-time response of COOH-MWCNTs FRP composite plates .....	24
Figure 26. Load-displacement response for various COOH-MWCNTs composite plates .....	25
Figure 27: Damage of FRP composites subjected to various levels of energy.....	26

## 2) The major goals of the project

The goal of the project is to develop the next generation of structural composites with enhanced impact-resistance capabilities over the current technology using carbon nanotubes (CNTs) and to understand the basic science behind this development. Our objectives include

- 1- Investigating basic methods to grow CNTs on the surface of carbon fabrics
- 2- Investigating basic methods to uniformly disperse CNTs in carbon fabrics
- 3- Investigating basic methods to fabricate carbon fabrics using CNTs
- 4- Mechanical characterization of the new composite including its impact strength
- 5- Understand the basic science behind its improved mechanical performance and impact strength.

## 3) What was accomplished under these goals?

Significant progress has been made in the last year. Our team successfully examined the significance of incorporating CNTs in the epoxy matrix. The objective of dispersing CNTs in the epoxy matrix was to prevent the inter-fiber fracture mode shown in **Figure 1**. A number of experiments to characterize the mechanical properties of CNTs-epoxy nanocomposite were performed. Moreover, on and Off-Axis testing of FRP composites incorporating CNTs was performed. We also tested the significance of CNTs on the lap splice of FRP composite. We acquired a new impact testing equipment and we started some preliminary impact testing on it. We plan to perform for extensive testing of impact strength of the new composites incorporating CNTs. A cost extension proposal for performing this testing plan will be submitted. Details of work performed are outlined in Item 4, 5 and 6 in this report. Page 2-20.

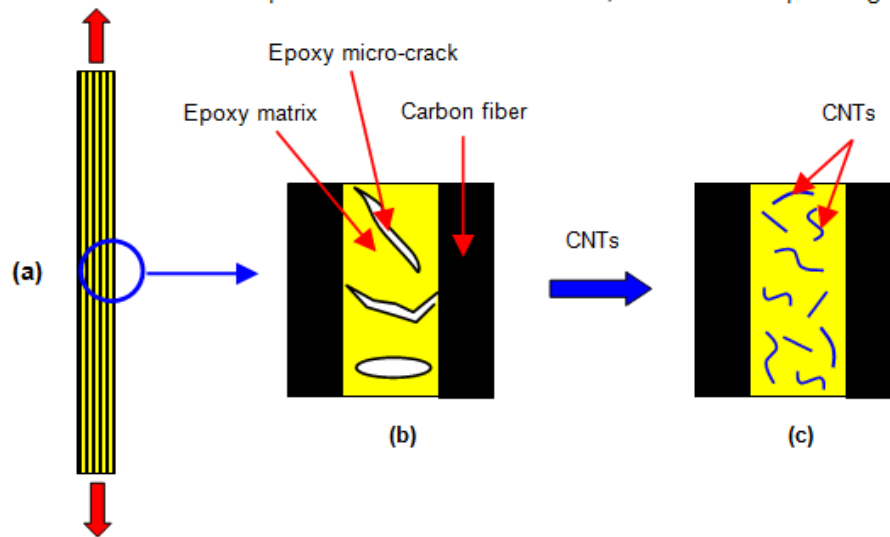


**Figure 1.** Schematic representation of CNTs mechanism in FRP composites (a) CFRP coupon subjected to tension force, (b) cohesive fracture of epoxy, and (c) CNTs reinforced epoxy composite.

### 3.1. Materials Properties

The carbon fiber fabric and the epoxy are supplied by U.S. Composites, Inc. The fabric is FG-CARB5750, balanced plain bidirectional (0-90°) weave, PAN based fiber, 3k tow size and 254  $\mu\text{m}$  thick with filament diameter of 1.0  $\mu\text{m}$ . The tensile strength of the raw carbon fibers is 4.48 GPa and the tensile modulus is 231 GPa. The bi-directional fabric is used here because it is adequate for the laboratory fabrication since the lateral threads provide lateral stiffness during the fabrication, and maintain the straight longitudinal threads. The plain weave fabric was selected over the other types of

weaves (i.e. twill or satin) because it provides the largest number of interlaces between the wrap and filling threads. Such large number of interlaces facilitates the fabrication process.

The epoxy used in fabrication is EPOTUF<sup>®</sup> 37-127 epoxy system. The epoxy resin is diluted liquid based on Bisphenol-A contains Diglycidyl ether (DGEBA) while the hardener is aliphatic Amine. The resin to hardener mixing ratio was 2:1, the pot life was 30-45 minutes at 80 °F (26.7 °C), the set time was 5-6 hours and curing time of 24-28 hours at room temperature. This type of epoxy has relatively low viscosity (600 cps) which facilitates the impregnation of the carbon fibers during the fabrication process. Furthermore, its pot life is relatively long to allow adequate time for the impregnation and the application of the vacuum environment before the epoxy partially hardens. The tensile strength and tensile elongation for the epoxy are 65 MPa and 25% respectively.

Pristine, surfactant treated, and functionalized MWCNTs were examined. The CNTs were supplied by Cheap Tubes, Inc. The outer diameter (OD) of the CNTs is 20-30 nm, the inner diameter (ID) is 5-10 nm and the length is 10-30 μm with an aspect ratio of 500 to 1000. The nanotubes were manufactured using catalytic chemical vapor deposition (CCVD) technique with purity being greater than 95% by weight. Two types of MWCNTs were supplied, pristine and functionalized with carboxyl groups (COOH). The functionalization was performed by the manufacturers using a mixture of non-organic acids. According to the manufactures, the functionalized MWCNTs had (COOH) functional groups of 1.23% by weight. The non-ionic surfactant Triton X-100 supplied by EMD chemicals was used for surfactant treatment. Triton X-100 has specific gravity of 1.065 at 25 °C, effective molarity of 1.7 M, viscosity of 240 cps at 25 °C, HLB value of 13.5, and critical micelle concentration (CMC) of 0.20 mM. Triton X-100 consists of a hydrophilic polyethylene oxide group (on average it has 9.5 ethylene oxide units) and a hydrophobic hydrocarbon group.

### **3.2. CNTs-Epoxy Nanocomposite Fabrication**

Four different types of treated epoxies were produced to fabricate the carbon woven composites in this study. The first type was neat epoxy prepared by mixing the resin with the hardener and applying the mixture directly to the carbon fabric during the impregnation process. The second type was prepared by reinforcing the epoxy with pristine MWCNTs. The dispersion was performed by adding the required MWCNTs content to the epoxy resin only and the CNTs-resin mixture was sonicated in ultrasonic bath for 1.0 hour at 40 °C. The reason for heating up the resin is to decrease the resin viscosity which helps in dispersing the nanotubes. The hardener was applied afterward to the CNTs-resin mix and the MWCNTs-epoxy nanocomposites were stirred and applied to the carbon fabric before curing.

The third type was prepared by reinforcing the epoxy with surfactant treated MWCNTs. In order to obtain 1.0% by weight MWCNTs-epoxy nanocomposite was produced by adding 500 mL methanol (solvent) to 1.0 g pristine MWCNTs and sonicating the mixture for 30 minutes. 0.6 g of the non-ionic surfactant Triton X-100 was added and the mixture was further sonicated for 2 hours. The weight-to-volume ratio (1.25 mg/mL) for the surfactant and solvent are chosen after Geng et al. (2008) and it is equivalent to 10 CMC. It can be noted that the surfactant content should exceed CMC in order to introduce strong steric repulsive forces among the nanotubes and it should not be very large to avoid the plasticizing effect of surfactant with low molecular weight. Epoxy resin of 100 g was heated to 75 °C under magnetic stirring using a hot plate and added to the CNTs-solvent-surfactant dispersion. The mixture was sonicated for 1.0 hour at 60 °C and vacuumed overnight to remove the solvent. The hydrophobic group (non-polar tail) of the surfactant would be attracted to the CNTs' surface creating non-reactive functional groups on the surface of the nanotubes. The hydrophilic group provides the

chemical compatibility with the epoxy matrix. The fourth type was prepared by reinforcing the epoxy with functionalized COOH-MWCNTs. The functionalized MWCNTs were added first to the resin and the mix was sonicated for 1.0 hour at 40 °C. In order to ensure chemical reaction between the functional groups on the surface of the nanotubes and the resin chains, the dispersed mixture was stirred for 2.0 hour at 80 °C. The hardener was added after cooling the resin and the epoxy-MWCNTs were further homogenized by mechanical mixing and then used in the composite fabrication. The functionalization process is shown in **Figure 2**.

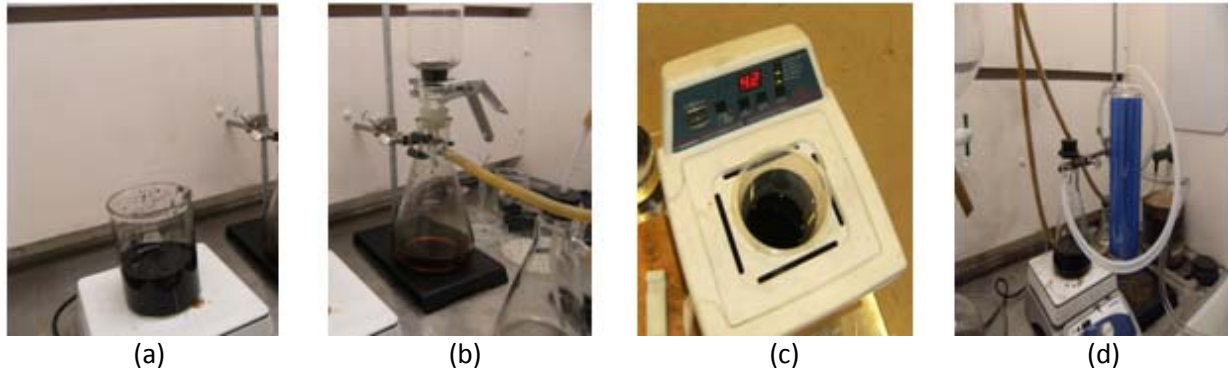


**Figure 2:** Functionalization of CNTs (a) Stirring of CNTs in acid mixture, (b) Filtration of functionalized CNTs, (c) Functionalized CNTs sonicated with solvent, and (d) Vacuum applied to remove solvent.

### **3.3. Fabrication of the CFRP Composite**

The fabrication of the CFRP composite was performed in accordance to ASTM D5687 standards. The vacuum assisted hand lay-up technique was implemented to fabricate the woven fabric composite sheets. Since the coupons loaded off-axially are expected to carry much lower load than the coupons loaded on-axially, six layers of fabric were used to fabricate the off-axis coupons while only two fabric layers were used to fabricate the on-axis test coupons. The number of fabric layers in the case of off-axis test was increased to achieve appreciable load carrying capacity for the off-axis test coupons. Peel plies, non-porous and porous release films, breather plies, and aluminum plate were used to ensure straight and compacted composite sheets and to facilitate peeling off the composite after curing. Adequate epoxy impregnation was achieved using roller and breather ply was placed to form the uniform air paths once the vacuum was applied. Same epoxy/carbon fabric weight ratio was used during the fabrication of all CFRP composites in order to maintain the same epoxy weight fraction. The epoxy weight fractions were obtained by measuring the change in weight between the original carbon fabric before and after epoxy impregnation. The epoxy weight fraction ranged between 30–33 %. The fabrication process of CFRP composites is shown in **Figure 3**.

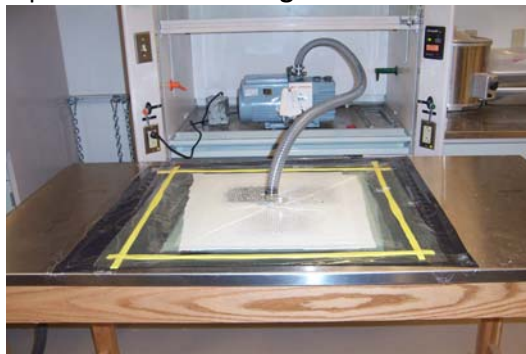


**Figure 3:** Fabrication of carbon fiber fabric using the vacuum assisted hand lay-up technique

For the rest of the article we will refer to the different epoxies used in the fabrication process as: neat epoxy (N), pristine CNTs reinforced epoxy (P), surfactant treated CNTs reinforced epoxy (S) and functionalized CNTs reinforced epoxy (F). It is important to note that the addition of CNTs increased the viscosity of the epoxy during the fabrication; therefore, limitation on the upper bound of the CNTs content was set to be 1.5% by weight. The vacuum bag contents were maintained at a vacuum level of  $2.3 \times 10^{-2}$  Torr for 24 hours to ensure full curing of the epoxy in the absence of air bubbles. A 1.0 mm thick CFRP tabs made from the same materials were attached to the ends of the composite coupons using epoxy in order to facilitate gripping the specimens in the testing frame and to avoid slip and possible failure at the grips.

### 3.4. On and off-axis tension tests

The off-axis tension test, where the loading direction was oriented at a 45° angle with respect to the fiber direction, was carried out according to ASTM standards D3518/D3518M-94. In this test, it is intended to examine the in-plane shear behavior of the CFRP composites. To compare the different types of MWCNTs on the off-axis tension behavior, only 1.0% CNTs by weight was examined and the different types of treated MWCNTs were compared with the reference case (neat epoxy). Five specimens were examined in each test as recommended by ASTM D3039. After analyzing the results, we did not pursue further the samples with surfactant treatment (S). Rather, we focused the rest of the investigation on the pristine (P) and functionalized (F) MWCNTs with a wider range of MWCNTs contents of 0.1, 0.5, 1.0 and 1.5 % by weight of epoxy. Off-axis tension testing was performed for these four MWCNTs contents. Moreover, on-axis tension test was performed, where the loading was oriented at the same direction as the fibers following ASTM D3039/D3039M-08 standards. In the on-axis tension test, the pristine (P) and functionalized (F) MWCNTs were examined with various contents including 0.1, 0.5, 1.0 and 1.5 % by weight. **Figure 4** shows the tension test setup.

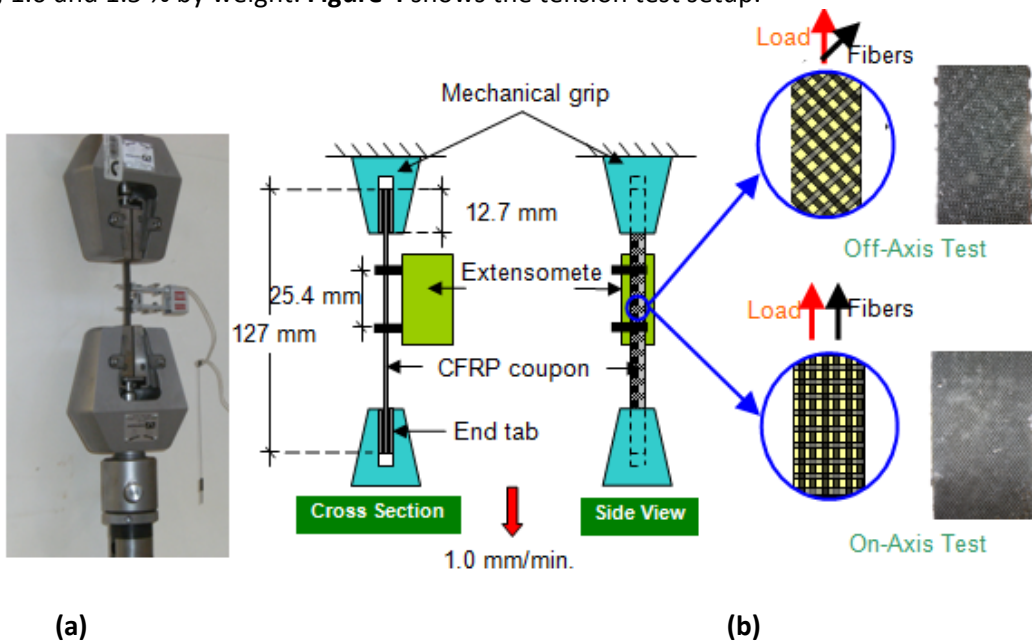


**Figure 4.** Tension test of CFRP composite (a) contact extensometer attached to CFRP coupons and (b) schematic for the test setup.

To further explain the experimental observations, the flexure behavior of various MWCNTs-epoxy nanocomposites was tested in four-point bending according to ASTM D6272-10 standards. 120 mm long, 15 mm wide, and 6 mm thick epoxy prisms were cast and tested with various CNTs loadings.

Moreover, the thermal analysis of MWCNTs-epoxy nanocomposites was examined using thermo gravimetric analysis (TGA) and scanning differential calorimetry (DSC) tests. The tests were performed with rate of 10 °C/minute over a temperature range of 25-1000 °C. Furthermore, the microstructure of various nanocomposites are investigated by scanning electron microscope (SEM).

Tension and flexure tests were performed on the coupons using MTS® Bionix servo hydraulic system. The machine has a load capacity of 25 kN and a maximum stroke of 130 mm. In each test, load, displacement, and strain were measured and recorded. The displacement was measured by the frame LVDT while the strain was measured by contact extensometer attached to the coupons with gauge length of 25.4 mm. The extensometer has +50% and -20% strain range which is much higher than failure strains typically observed in FRP composites. The sampling rate for all the experiments was 50 Hz and the data was collected by FlexStar MTS® 793 data acquisition system. For each coupon, the stress-strain relation was obtained. The tensile strength, Young's modulus, failure strain, and toughness were then evaluated and compared. The tensile toughness was computed from the area under the stress-strain curve and it indicates the ability of the material to absorb energy before failure. This shall not be confused with fracture toughness which requires testing of notched specimens. Statistical analysis was performed on test results and the statistical significance of difference between the specimens was evaluated using the student t-test assuming 95% levels of significance.

Failure behaviors of on- and off-axis tests are shown schematically in **Figure 5**. Microscopic images in Figure 5 show that on-axis coupons failed by longitudinal fiber fracture with limited damage in the epoxy matrices. This failure behavior is typically observed when composites are loaded along the fiber direction. The failure indicates that the composites tensile behavior is dominated by the fibers and the matrix contribution in on-axis tension is limited. On the other hand, two observations can be deduced from the off-axis failure (Figure 5). Severe epoxy damage occurred at the failure zone including excessive delamination due to inter-fiber fracture. In addition, no fiber fracture is observed in the off-axis coupons. Furthermore, the effect of failure behavior on the stress-strain curve is schematically explained in **Figure 5**. The reduction in Young's modulus as the stress increased indicates composite matrix damage caused by inter-fiber fracture. Almost no change in Young's modulus was observed for the on-axis tested samples while significant change was observed for the off-axis tested ones.

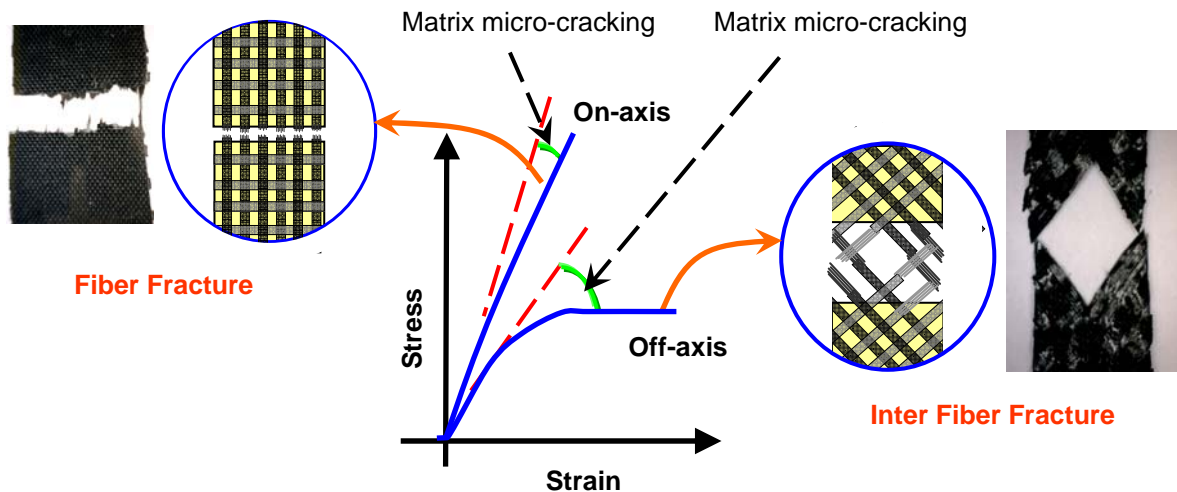


**Figure 5.** Failure mechanism for on and off-axis CFRP coupons.

The off-axis stress strain response for various types of MWCNTs-epoxy FRP composites with 1.0% by weight MWCNTs content are presented in **Figure 6** and the statistical analysis of the five replicates is

reported in **Table 1**. The figure shows a sample of two coupons from each group. Significant decrease in all tensile properties was observed for the composites incorporating surfactant-treated (S) MWCNTs. Young's modulus, ultimate strength, and toughness decreased by 58%, 24% and 43%, respectively, compared with the corresponding values for composite based on the neat epoxy (N). However, no change was observed in the failure strain. The pristine (P) MWCNTs case showed increase in the failure strain and toughness by 29% and 16%, respectively, though, no increase in ultimate strength was observed. The functionalized MWCNTs (F) showed 20% increase in both ultimate strength and failure strain and 50% increase in toughness.

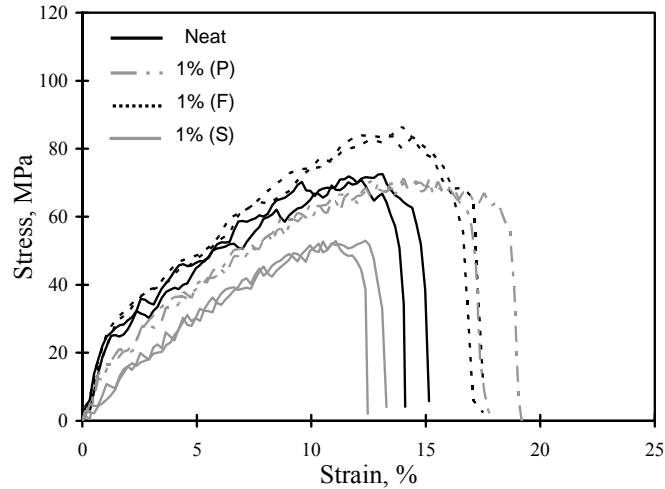


**Figure 6.** Stress-strain relationships for CFRP off-axis composite coupons for various chemical treatments of 1.0% MWCNTs-epoxy nanocomposites.

**Table 1.** Statistical analyses for off-axis test coupons with various chemical treatments of 1.0% CNTs presenting modulus of elasticity (E), ultimate strength ( $\sigma_u$ ), failure strain ( $\epsilon_f$ ) and Toughness (T).

		E (GPa)	$\sigma_u$ (MPa)	$\epsilon_f$ %	T (MPa.mm/mm)
Neat	Mean	3.86	69.8	14.45	6.67
	STD <sup>†</sup>	0.84	2.86	1.0	0.71
1.0% (P*)	Mean increase) ( $\pm$ %)	3.54 (-8%)	71.2 (2%)	18.57 (28%)	7.76 (16%)
	STD	0.98	3.06	0.91	0.54
1.0% (F**)	Mean increase) (%)	4.63 (20%)	83.8 (20%)	17.31 (20%)	10.03 (50%)
	STD	0.74	1.84	0.74	0.75
1.0% (S§)	Mean increase) (%)	1.61 (-59%)	53.21 (-24%)	14.47 (0.1%)	3.77 (-44%)
	STD	0.25	0.32	1.43	0.4

\*P: Pristine, \*\*F: Functionalized, §S: Surfactant treated, <sup>†</sup>STD: standard deviation,  $\pm$ % Increase: percentage of increase

**Figure 7 (a)** depicts the stress-strain response for the pristine (P) MWCNTs case with various % wt MWCNTs contents. In addition, statistical analysis for the off-axis test is presented in Table 2. The highlighted cells in **Table 2** correspond to the cases discussed in this section. From **Figure 7 (a)**, it is

noted that the pristine (P) MWCNTs have significant effect on the failure strain. For example, the strain increase due to the addition of 0.1, 0.5, 1.0, and 1.5 % (P) MWCNTs were 13, 18, 28 and 30 % respectively. However, limited effect on ultimate strength is observed with the highest increase of 10% associated with 0.5% (P) MWCNTs. The moderate improvements in failure strains, associated with the addition of pristine MWCNTs (P), can be attributed to the CNTs ability to provide some crack barrier effect within the matrix at the nanoscale and thus enabling the epoxy matrix to continue carrying loads after cracking.

**Table 2.** Statistical analyses for off-axis test coupons presenting modulus of elasticity (E), ultimate strength ( $\sigma_u$ ), failure strain ( $\epsilon_f$ %) and Toughness (T).

		E (GPa)	$\sigma_u$ (MPa)	$\epsilon_f$ %	T(MPa.mm/mm)
Neat	Mean	3.86	69.8	14.45	6.67
	STD†	0.84	2.86	1.0	0.71
0.1% (P*)	Mean (‡% increase)	3.74 (-3%)	66.9 (-4%)	16.4 (13%)	7.17 (7%)
	STD	0.56	6.36	0.9	0.54
0.5% (P)	Mean (% increase)	4.29 (11%)	76.6 (10%)	17.12 (18%)	7.94 (19%)
	STD	0.91	4.72	0.67	0.64
1.0% (P)	Mean (% increase)	3.54 (-8%)	71.2 (2%)	18.57 (28%)	7.76 (16%)
	STD	0.98	3.06	0.91	0.54
1.5% (P)	Mean (% increase)	3.63 (-6%)	69.6 (-0.3%)	18.70 (30%)	7.69 (15%)
	STD	0.92	2.78	0.94	0.53
0.1% (F**)	Mean(% increase)	4.56 (18%)	67.4 (-3%)	15.39 (6%)	7.07 (6%)
	STD	0.92	2.9	1.08	0.37
0.5% (F)	Mean (% increase)	4.35 (13%)	79.1 (13%)	14.57 (1%)	8.04 (21%)
	STD	0.81	3.0	0.89	0.72
1.0% (F)	Mean (% increase)	4.63 (20%)	83.8 (20%)	17.31 (20%)	10.03 (50%)
	STD	0.74	1.84	0.74	0.75
1.5% (F)	Mean (% increase)	3.85 (-.3%)	97.1 (39%)	21.81(51%)	14.72 (121%)
	STD	0.91	3.79	1.24	1.44

\*P: Pristine, \*\*F: Functionalized, †STD: standard deviation, ‡% Increase: percentage of increase

The FRPs samples containing functionalized (F) MWCNTs exhibited significant increase in ultimate strength, failure strain, and toughness as shown in **Figure 7 (b)**. 20 and 39 % enhancements in ultimate strength were achieved by adding 1.0 and 1.5 % (F) MWCNTs, respectively. Also, 20 and 50 % improvements in failure strains were achieved with the same content of the functionalized MWCNTs. The increase in toughness reached 121% with 1.5% (F) MWCNTs. It is obvious that the functionalized MWCNTs increased the failure strain further and enhanced the ultimate strength significantly. The role of functionalizing the MWCNTs in increasing the interfacial bond between the nanotubes and the epoxy matrix and enhancing the tensile response is evident. Unlike ultimate strength, failure strain, and toughness, limited modification in Young’s modulus was observed. The highest increase in Young’s modulus of elasticity is limited to 20% as observed in the case of 1.0% (F) MWCNTs.

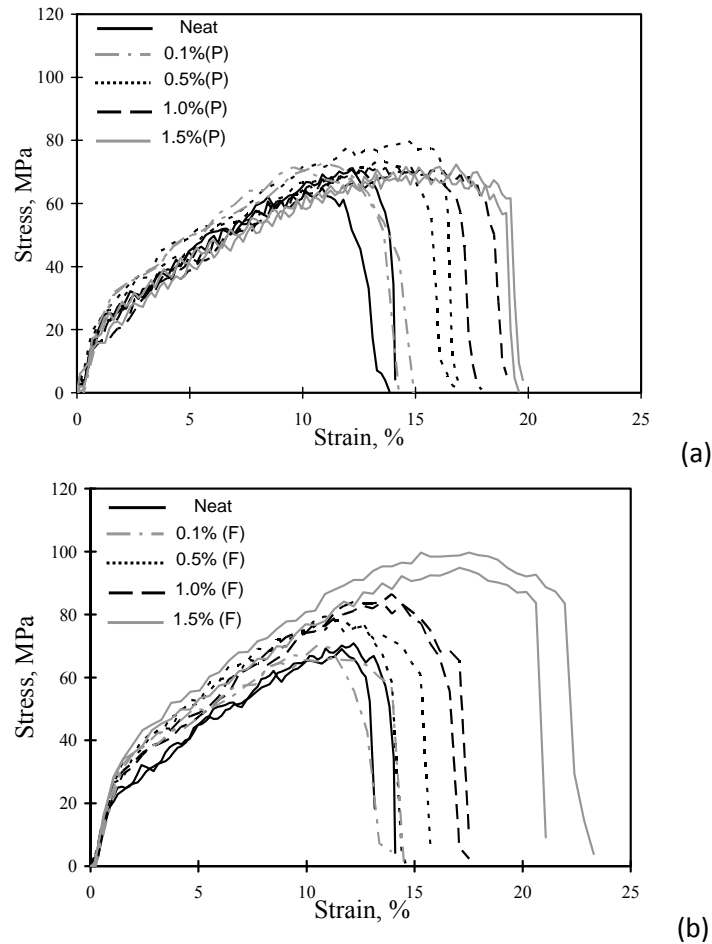


**Figure 7.** Stress-strain relationships for CFRP off-axis composite coupons with various MWCNTs-contents: (a) pristine (P) and (b) functionalized (F).

**Figure 8** shows the on-axis stress-strain behavior of FRPs composites based on pristine (P) and functionalized (F) MWCNTs and the statistical analyses for both cases are reported in Table 3. The highlighted cells in Table 3 correspond to the cases discussed in this section. In general, limited effect on the on-axis tensile properties was observed when pristine (P) or functionalized (F) MWCNTs were used as oppose to the off-axis properties. This effect includes both increase and decrease in tensile properties. For example, toughness improvements of 20 and 29 % were observed for the case of 0.5 and 1.0 % (F) MWCNTs respectively. Also, toughness increases of 6 and 5 % were reported for the samples with 0.1 and 1.0 % wt (P) MWCNTs respectively. On the contrary, decreases in toughness of 17 and 2 % were also observed in cases of 0.5% (P) and 1.0% (F) MWCNTs respectively. These observations were consistent to other tensile properties such as ultimate strength and failure strain as well.

**Table 3.** Statistical analyses for on-axis test coupons presenting modulus of elasticity (E), ultimate strength ( $\sigma_u$ ), failure strain ( $\epsilon_f$ ) and Toughness (T).

		E (GPa)	$\sigma_u$ (MPa)	$\epsilon_f$ %	T (MPa.mm/mm)
Neat	Mean	40	554	1.38	3.8
	STD,	2.8	36.56	0.11	0.56
0.1% (P)	Mean (% increase)	47 (17%)	543 (-2%)	1.39 (0%)	4.02 (6%)
	STD,	6.72	20.63	0.17	0.51
0.5% (P)	Mean (% increase)	41 (1%)	493 (-11%)	1.18 (-14%)	3.16 (-17%)
	STD,	1.8	83.32	0.14	0.62
1.0% (P)	Mean (% increase)	44 (9%)	607 (10%)	1.32 (-5%)	4 (5%)
	STD	2.64	60.7	0.16	0.89
1.5% (P)	Mean (% increase)	43 (6%)	591 (7%)	1.34 (-3%)	3.88 (2%)
	STD	2.97	30.73	0.08	0.34
0.1% (F)	Mean (% increase)	40 (-1.5%)	630 (14%)	1.50 (9%)	4.58 (20%)
	STD	2.4	47.25	0.15	0.63
0.5% (F)	Mean (% increase)	40 (-0.1%)	620 (12%)	1.59 (13%)	4.91 (29%)
	STD	1.76	94.86	0.31	1.43
1.0% (F)	Mean (% increase)	39 (-3%)	548 (-1%)	1.37 (-1%)	3.71 (-2%)
	STD	2.34	50.96	0.09	0.6
1.5% (F)	Mean (% increase)	38 (-5%)	556 (0%)	1.34 (-3%)	3.97 (4%)
	STD	2.58	108.42	0.27	1.14

\*P: Pristine, \*\*F: Functionalized, †STD: standard deviation, ‡% Increase: percentage of increase

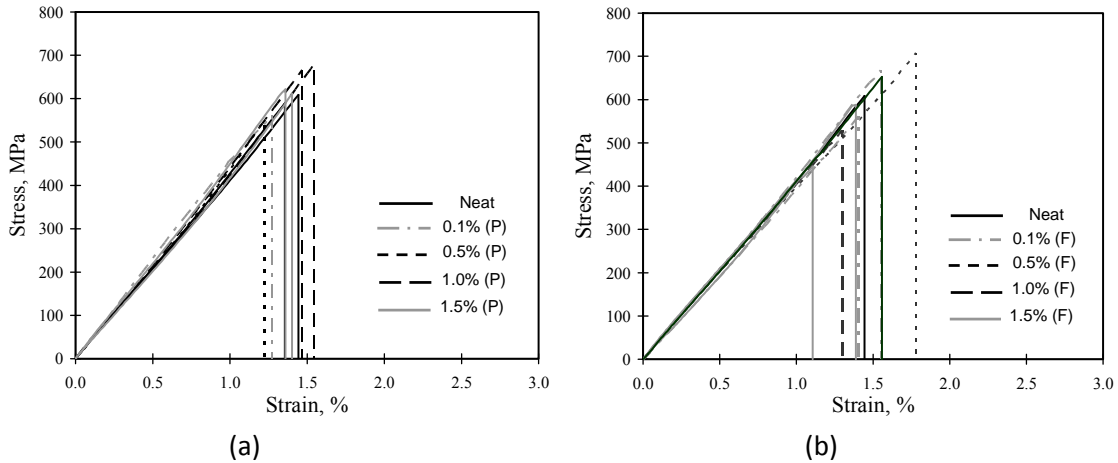


**Figure 8.** Stress-strain relationships for CFRP on-axis composite coupons with various MWCNTs-contents: (a) pristine (P) and (b) functionalized (F).

The tensile toughness is chosen as a sample to demonstrate the difference in CNTs effect on the on and off-axis tests. **Figure 9** depicts a bar chart comparison for the normalized toughness between the on and off axis tests for various CNTs contents. In this figure the toughness is normalized with respect to the neat epoxy case. Statistical analyses show that there are no significant differences in toughness among various cases for CNTs contents in the on-axis test. On the contrary, there are significant statistical differences in toughness between various CNTs contents in the off-axis test. Moreover, the

effect of CNTs on toughness is nonlinear and increases significantly with the addition of CNTs. In general, the changes in tensile properties in on-axis tests are lower than that observed in the off-axis test. This could be explained by the fact that fibers dominate the tensile behavior of the coupons when loaded in the on-axis direction. Failure occurred mainly due to fiber fracture and very limited matrix damage was observed under on-axis loading.

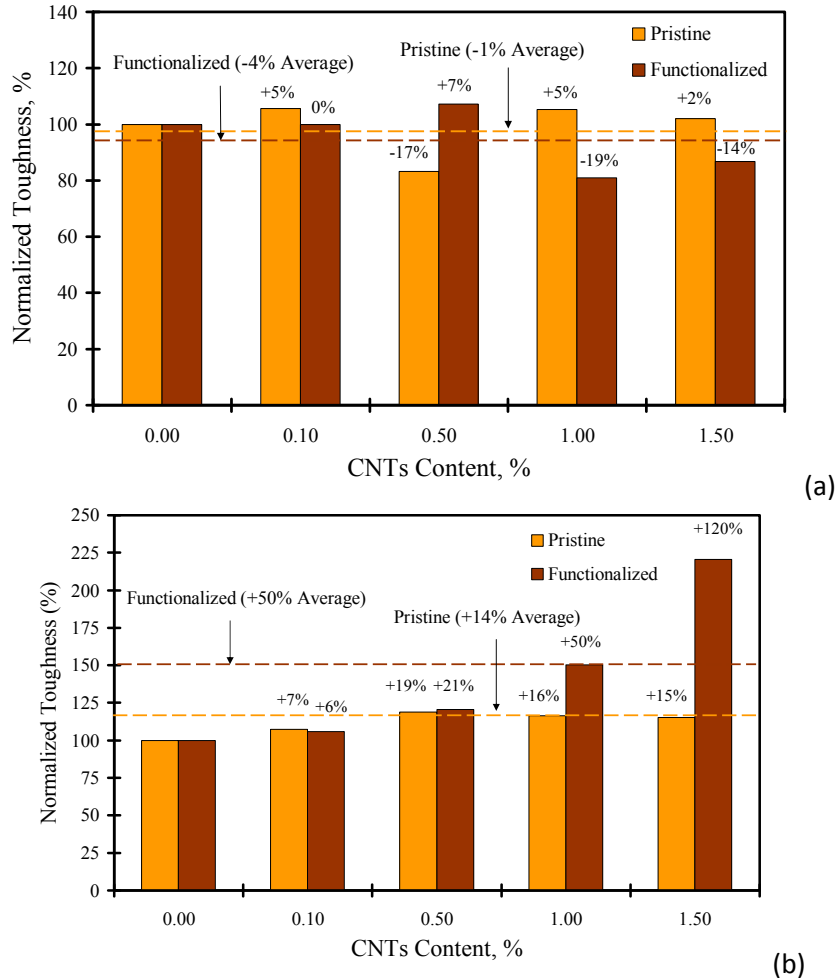


**Figure 9.** Normalized tensile toughness for CFRP composites coupons with various MWCNTs-contents: (a) on-axis and (b) off-axis.

### 3.5. Flexure test

The results of the flexure test on MWCNTs-epoxy nanocomposites are shown in **Figure 10**. The maximum bending stress and strain are computed for 1.0% MWCNTs for the three cases; pristine (P), functionalized (F) and surfactant treated (S) MWCNTs. The neat epoxy exhibited average ultimate strength and bending modulus of 20.9 MPa and 0.910 GPa respectively. The pristine (P) MWCNTs exhibited limited increase in strength and modulus of 8.5 and 5.9 % respectively. The failure strain was not examined due to ASTM standards limitations on the maximum strain in bending test. A noticeable decrease in strength and modulus of 24 and 13 % were observed for the samples based on surfactant treated (S) MWCNTs. The flexure results of the surfactant treated MWCNTs explain the poor behavior in the FRP composite coupons incorporating surfactant treated (S) MWCNTs. Two reasons might lead to the mechanical degradation of the surfactant treated MWCNTs-FRP composites. The first reason could

be the difficulties in completely removing all the solvent during the processing of surfactant treated MWCNTs-epoxy nanocomposite. Remaining solvent molecules could have adverse effect on epoxy hardening process and thus on the mechanical properties of the nanocomposite. The remaining solvent molecules, if exist, would affect the thermal stability of the nanocomposites in the TGA and DSC tests. Another reason could be the content of surfactant in the epoxy matrix. Although similar surfactant concentration (10 CMC) was used by Geng et al. and is proven to enhance the mechanical response of the CNTs-epoxy nanocomposites; however, the types of epoxy resin used in the two studies are different. In this study, the relatively large content of surfactants affected adversely the mechanical performance of the nanocomposites due to their low molecular weight and plasticizing effect. On the contrary, the functionalized (F) MWCNTs-epoxy significantly enhanced the strength and Young's modulus of the epoxy by 43 and 40 % respectively. The increase in strength and stiffness is attributed to the strong interfacial bond that takes place between the MWCNTs and the surrounding epoxy matrix. Covalent attachment of functional groups to the surface of nanotubes has a higher efficiency for load transfer and offers the opportunity for chemical interactions with the epoxy systems. The strength improvement of the nanocomposite confirms the results of the off-axis test coupons.

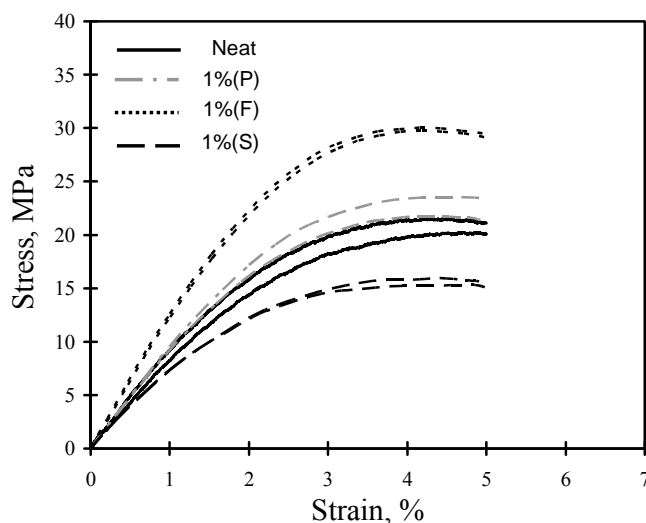


**Figure 10.** Bending stress-strain relationships for various MWCNTs-epoxy nanocomposites.

### 3.6. Thermal stability

The objective of the TGA test is to investigate the effect of incorporating MWCNTs on the decomposition point of the epoxy nanocomposites. The decomposition of materials occurs as a result of chemical bond break. Therefore, the existence of covalent bonds between the functionalized MWCNTs and the surrounding matrix can be identified by comparing the TGA of the pristine and functionalized MWCNTs-epoxy nanocomposites. On the other hand, the DSC is performed to investigate the heat required to increase the temperature of various CNTs-epoxy nanocomposites measured by the heat flow. In addition, the TGA and DSC tests give indication about the presence of solvent molecules in the nanocomposites. **Figure 11** shows the normalized heat flow of various MWCNTs-epoxy nanocomposites measured by DSC test. For comparison purpose, the heat flow values at 200°C are reported and compared for various nanocomposites. The normalized heat flows at 200°C were 4.85, 1.75, 0.83, 0.64, and 0.62 mW/mg corresponding to functionalized (F), Surfactant treated (S), Neat (N) and Pristine (P) MWCNTs-epoxy nanocomposites. The individual nanotubes absorb the largest amount of heat followed by the functionalized MWCNTs-epoxy nanocomposites. The heat flow of the surfactant treated

MWCNTs-epoxy nanocomposites indicates the solvent molecules in the nanocomposites are fully evaporated. This observation also leads to the assumption that the degradation of the mechanical properties of surfactant treated FRPs coupons is likely due to the relatively large content of surfactant. Although the same amount of surfactant reported by Geng et al. (2008) of 10 CMC is used here, the results observed in this study are contradicting with the results reported by Geng et al. (2008). This might be attributed to the inadequate dispersion of surfactant and nanotubes and/or to the difference in the types of epoxy resins used in the two studies.

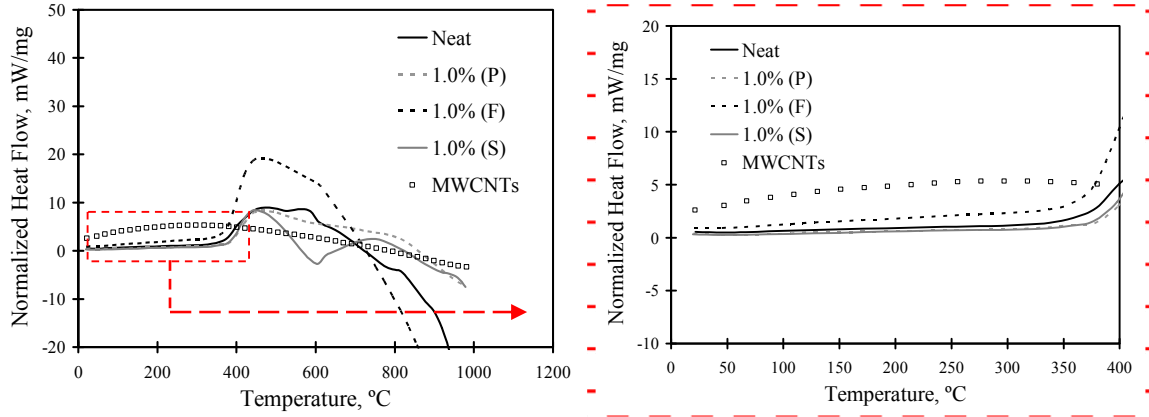
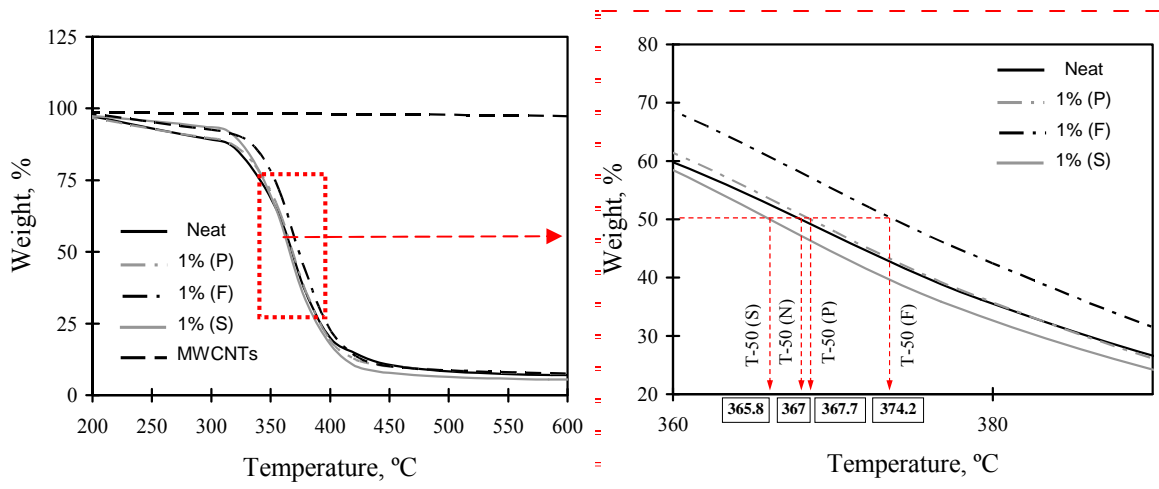


Figure 11. DSC results for various MWCNTs-epoxy nanocomposites.

Figure 12 shows the TGA plots for the MWCNTs and the MWCNTs-epoxy nanocomposites. In the TGA, the temperature (T-50), at which 50% of the weight diminishes, was reported and compared for the different samples as an indication for material decomposition. The nanotubes showed outstanding thermal stability and T-50 was not observed within the examined range. T-50 for the neat (N), pristine (P), functionalized (F), and surfactant treated (S) MWCNTs-epoxy nanocomposites were 367.0, 367.7, 374.2 and 365.8 °C respectively. Since, the nanotubes have high thermal stability; it is expected to enhance the thermal stability for the neat epoxy matrix. However, the surfactant treated (S) case showed a slight decrease of 1.2 °C in T-50, which confirms the absence of solvent molecules in the nanocomposites. The pristine (P) case exhibited limited increase of 0.7 °C of T-50 due to the absence of chemical bonds between the MWCNTs and the epoxy matrix. The functionalized (F) case showed 7.2 °C increase in T-50 due to the strong interfacial bond between the nanotubes and the epoxy matrix. The strong interfacial bond requires more energy (higher temperature) to break; thus the epoxy with functionalized MWCNTs showed higher T-50 than the one with pristine (P) MWCNTs. TGA observations, therefore, confirm the improved bond between functionalized MWCNTs and the epoxy matrix compared with the bond between pristine MWCNTs and epoxy matrix.



**Figure 12.** TGA results for various MWCNTs-epoxy nanocomposites.

### 3.7. Microstructural investigation

SEM surface images with the same magnification for 1.0% by wt. MWCNTs with various surface conditions are shown in **Figure 13**. By comparing the difference between the high magnification epoxy nanocomposite images [**Figure 13 (b-d)**], one can identify the nanotubes as bright spots. The dispersion for the nanotubes for the pristine [**Figure 13 (b)**] and functionalized [**Figure 13 (c)**] MWCNTs seems to be proper and the scatter of the nanotubes is fairly uniform. This indicates that the mixing techniques are appropriate to disperse the nanotubes in the low viscosity epoxy resin used. However, it is quite difficult to identify the nanotubes in the case of surfactant treated MWCNTs [**Figure 13 (d)**]. In addition, large regions of surfactant micelles (appears as dark areas) seem to form in the case of surfactant treated MWCNTs-epoxy nanocomposites as shown in the low magnification SEM images [**Figure 13 (e-f)**]. It is expected that these regions enclose the nanotubes interacted with the surfactant. The relatively large content of surfactant used here resulted in the formation of large micelles which adversely affected the mechanical performance of the nanocomposites.

It is evident from the above investigation that incorporating functionalized MWCNTs can significantly improve the shear strength and failure strain of the FRP composites (up to 39% for strength and 51% of failure strain using 1.5% (F) MWCNTs by weight). This finding can be significant for the FRP composite industry. A recent market investigation by the authors showed that addition of 1.5% MWCNTs in epoxy matrix might lead to 20% increase in the FRP composite fabrication cost. This is a limited cost increase with the significant shear strength and strain increases listed above. Potential applications for this research would be the cases where FRP composite behavior is governed by shear strength of the polymer matrix. Example applications include multi-axially FRP laminates loaded in many directions due to blast or seismic events. The use of functionalized MWCNTs might also be useful in enhancing shear strength of FRP bolts and shear studs, enhancing shear strength of FRP pultruded sections always governed by limited shear strength of FRP and enhancing shear strength of FRP prestressing strands in anchorage zones which is a major problem in FRP prestressing. Further research is warranted in these fields to showcase the benefits of using CNTs on producing a new generation of FRP with enhanced shear strength.

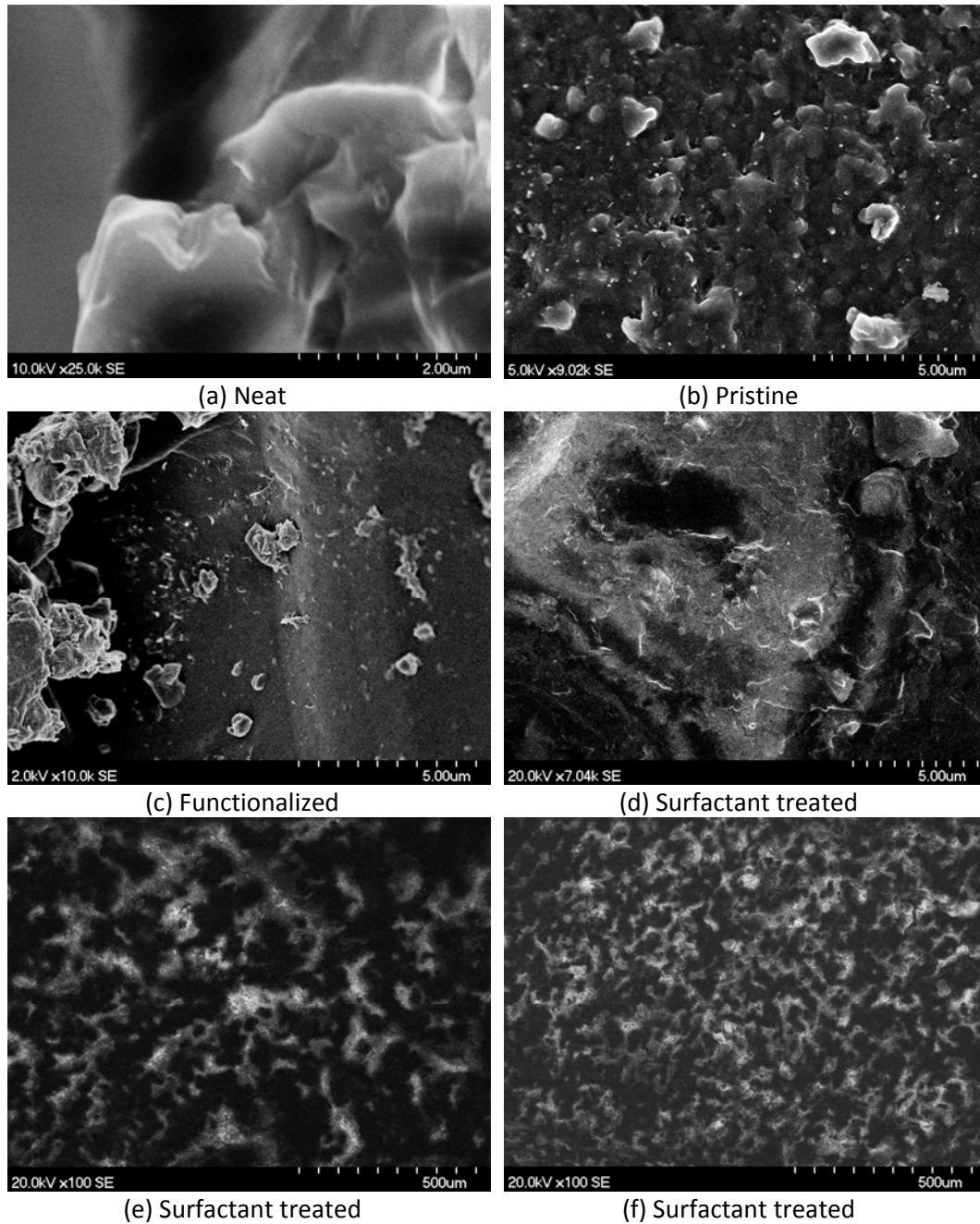


**Figure 13.** SEM images for CNT-epoxy nano-composites with various CNTs surface conditions (a-d) high magnification and (e-f) low magnification images

### 3.8. Lap shear splice characterization

There are several ASTM standards for testing single lap shear specimens in order to obtain adhesive shear properties for thin substrates with different materials. All of these standards share similar challenges when obtaining true shear properties as oppose to apparent properties. It is observed and reported that single lap shear joints rotate when subjected to uniaxial tension. The rotation of the joint

causes bending and peel or cleavage stresses in addition to the pure shear stresses. In this context, ASTM D4896 distinguished between apparent and true bond strengths. There are two methods to overcome the secondary deformations. First, the use of thick adherent specimens as proposed by ASTM D3983 and ASTM D5656. The thick adherent would limit the rotation of the joint and therefore would minimize secondary effects at the joint. The second method is to use double lap shear joint for thin adherents as proposed by ASTM D3528 . The ASTM standard proposes two configurations for the double lap shear test as shown in **Figure 14**. The symmetry in the geometry of the double lap joint eliminates the secondary deformations and the normal stresses. In this study, the configuration in Figure 14 (a) was used to estimate the shear/bond strength of MWCNTs-epoxy nano-composites.

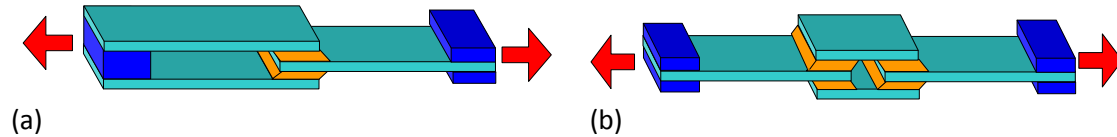


**Figure 14.** Double lap joint configurations

The lap surface was 19 mm × 12.7 mm prepared by grinding the CFRP composite surface with Grit 80 first coat drywall sand paper. 0.5% by volume glass beads with  $0.71 \pm 0.035$  mm diameter, provided by Mo-Sci Corporation, were added to the CFRP lap surface in order to control the CNTs-epoxy composite thickness as recommended by ASTM standards. The prepared CNTs-epoxy nanocomposite was cast on the lap surface via syringe pump to avoid any formation of voids and the excess of epoxy was carefully removed. A proper lateral pressure was applied to the joint surface using electrical clamps and the CNTs-epoxy nanocomposite was cured for 14 days prior to testing. The specimens were then tensioned until failure using displacement-controlled mode with rate of 0.5 mm/minute. Five specimens were tested for each MWCNTs loading and the statistical analysis using student t-test was performed with 95% level of confidence. The lap joint test was performed using MTS<sup>®</sup> Bionix servo hydraulic system and an extensometer was used to record the axial deformations at the joint (**Figure 15**). The epoxy shear strain  $\gamma$  for the lap joint is computed as  $\gamma = \Delta L/h$  where  $h$  is the bondline thickness (0.71 mm), and  $\Delta L$  is the shear slip measured by the extensometer. In addition, the shear stress  $\tau$  acting on the shear joint can be computed as  $\tau = P/2A$  where  $A$  is the area of the lap joint and  $P$  is the applied load.

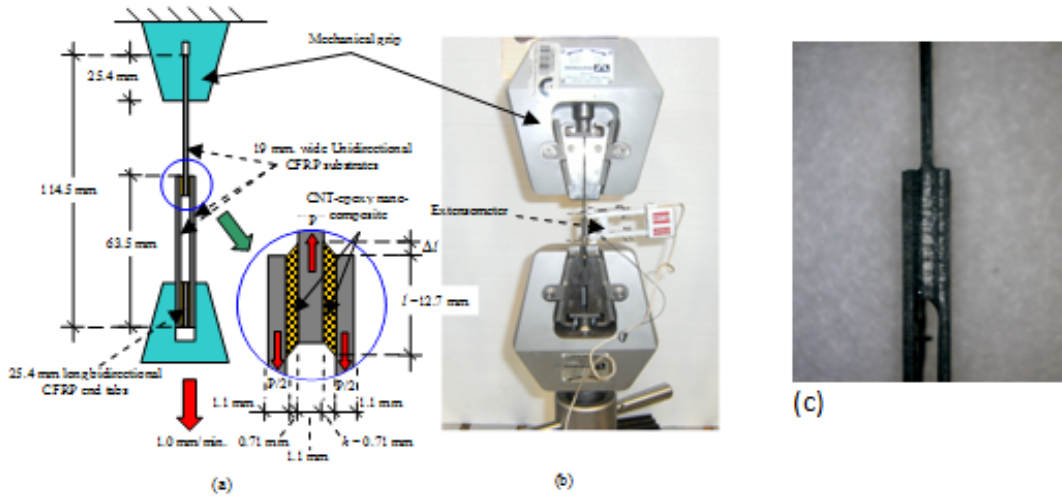


**Figure 15.** Double lap joint test setup (a) joint dimensions, (b) extensometer attached to the joint, and (c) close view for the lap joint

All specimens failed at the epoxy-FRP interface and the two sides of the double lap joint failed simultaneously. The test results are therefore adequate to evaluate the bond strength for various epoxy nanocomposites. The shear stress-strain curves for the lap joint tests are shown in **Figure 16**. Only two specimens from each MWCNTs loading are shown however, the statistical analysis is performed for all specimens. The figure shows that when neat epoxy or 0.5% MWCNTs is used to splice the FRP strips, the behavior of the joint is linear until failure. However, the lap joints with 1.0 and 1.5% MWCNTs loadings showed nonlinear behavior. The difference in the behavior between the specimens can be attributed to the significance of high MWCNTs contents: 1.0 and 1.5%. High contents of the MWCNTs were able to produce nonlinear shear behavior of FRP lap splice providing enhancement in failure shear strain and energy absorption to failure.

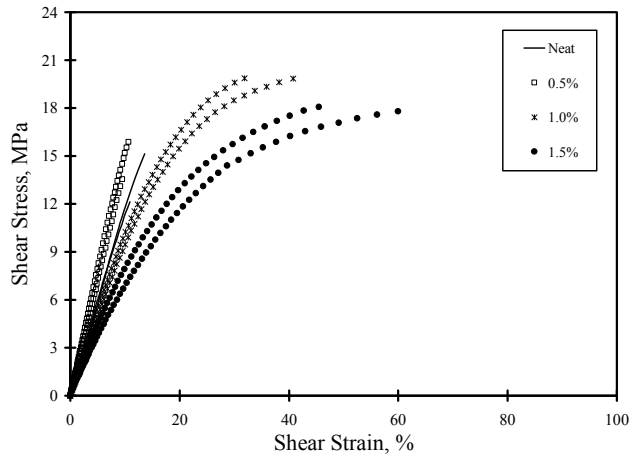


**Figure 16.** Shear stress-strain of FRP lap splice with various MWCNTs loadings

The average shear moduli were  $141 \pm 65$ ,  $173 \pm 27$ ,  $109 \pm 40$ , and  $92 \pm 7$  MPa for the 0, 0.5, 1.0, and 1.5% MWCNTs-epoxy nanocomposites respectively. The statistical analyses using student t-test indicate that there is no significant statistical difference in the shear moduli among all cases. In addition, the bond strengths for the four cases were  $11.8 \pm 3.9$ ,  $14.3 \pm 2.2$ ,  $15.1 \pm 2.77$ , and  $16.2 \pm 2.6$  MPa respectively. It was found that there is no statistical difference in the bond strength between the neat and 0.5% MWCNTs cases. However, there is significant difference between the neat epoxy and epoxy nanocomposite incorporating 1.0 or 1.5% MWCNTs. The bond strength increased by 49% and 37% with the addition of 1.0 and 1.5% MWCNTs. **Figure 17 (a)** shows that the optimal content of the MWCNTs for improving the bond strength is 1.0%. The mechanism of improving the bond strength can be understood through **Figure 1** where the CNTs become part of the epoxy microstructure and therefore contribute in shear load carrying capacity and enhance the matrix shear strain at failure.

Furthermore, the failure strains were 9.2, 8.6, 26, and 42% due to the addition of 0, 0.5, 1.0, and 1.5% MWCNTs respectively. Similar to the bond strength, the statistical analyses showed significant increase in shear strains at failure only between the neat epoxy and the 1.0 or 1.5% MWCNTs loadings. The enhancement in failure shear strains reached 187 and 360% with 1.0 and 1.5% MWCNTs respectively (**Figure 17 (b)**). Previous experimental and numerical studies showed that MWCNTs have high tensile elongation of 10-20% which could explain the significant increase in failure strain of the MWCNTs-epoxy nanocomposite. Since toughness can be measured by the area under the stress-strain curve, toughness combines the improvements in both the stress and strain levels. In this study, the enhancement in toughness reached 700 and 1130 % for the case of 1.0 and 1.5% MWCNTs. The reported enhancements

are significant and can be used to enhance the performance of FRP lap splice in applications governed by energy absorption such as seismic retrofit of reinforced concrete (RC) structures using FRP.

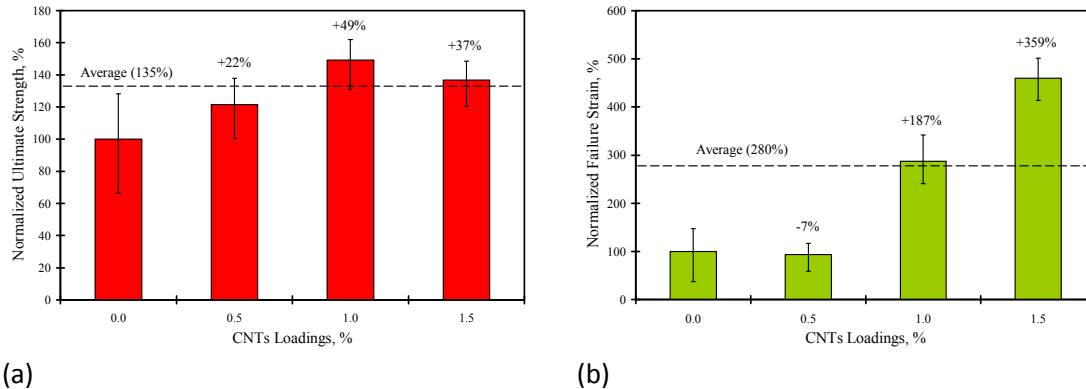


**Figure 17.** Comparison of (a) shear strength (b) failure strain for different MWCNTs epoxy nanocomposites.

Finally, the ACI 440.2R for external strengthening RC structures with FRPs does not provide direct methods for computing lap splice length. The provisions instead refer to the manufacturers' specifications and experimental testing to determine the appropriate lap splice length. This might be attributed to the variability in the FRP and adhesive material properties and/or because there is not enough experimental data to establish consistent design requirements for FRP lap splice length. In general, the lap splice should be long enough to transfer the stresses among the spliced FRP laminates. Since 1% MWCNTs can obviously improve the bond strength in FRP lap splice by about 50%, CNTs can provide promising technique to shorten FRP lap splice length or the bonded area to one half. This technique would be beneficial where the strengthened area is of limited space such as in seismic retrofit of RC beam–column joints. More interestingly is the strain capacity and toughness which are strongly required for seismic retrofit. The relatively small loadings of CNTs needed to achieve such enhancements in FRP lap splice make it attractive to use CNTs in such applications.

### 3.9. Fracture Toughness Testing

Furthermore, the interlaminar fracture toughness of CFRP composites incorporating CNTs were examined. MWCNTs functionalized by carboxyl (COOH) groups are used to improve mode I interlaminar fracture toughness of epoxy/carbon woven composites. The significance of the carboxyl (COOH) functionalization group on interlaminar fracture toughness of epoxy/carbon woven composites has not been reported before. Investigations by the research team showed that the use of COOH-MWCNTs improved the off-axis tension (i.e. shear) strength and strain of the woven fabric composites by 39% and 51% respectively. These improvements in the tensile and impact response can be attributed to enhanced interlaminar fracture toughness. This article demonstrates this observation using double cantilever beam (DCB) tests.

The fabrication of the DCB specimens was performed in accordance to ASTM D5687 standards. The vacuum assisted hand lay-up technique was implemented to fabricate the woven fabric composite sheets. Twelve fabric layers were used to fabricate the DCB specimens. The same epoxy/carbon fabric weight ratio was used during the fabrication of all specimens in order to maintain the same fiber volume fraction. Release film, 15  $\mu\text{m}$  thick, was inserted during the fabrication at the mid height in order to create the initial crack. The initial crack length was 32 mm. The DCB test setup is shown in **Figure 18**. The

test was conducted according to ASTM D5528 [23]. Three specimens were tested for each MWCNTs loading. Once the load was applied in a displacement controlled mode with rate of 0.5 mm/minute, the load  $P$ , the opening displacement  $\delta$  and delamination length  $a$  were recorded by the MTS load cell, contact extensometer, and in-situ optical microscope, respectively, as shown in **Figure 18**. Mode I critical energy release rate,  $G_{Ic}$ , is computed using modified beam theory (MBT) as given in Eq. (1).

$$G_{Ic} = \frac{3P\delta}{2b(a + \Delta)} \quad (1)$$

where  $P$  is the applied load,  $b$  is the specimen width,  $a$  is the delamination or crack length,  $\delta$  is the opening displacement in DCB test, and  $\Delta$  is a correction for the delamination length. The MBT assumes that linear elastic fracture mechanics (LEFM) applies because the size of the fracture process zone is much less than the thickness of the specimen. As the displacement increases, the delamination grows until a steady-state growth is obtained. The steady-state delamination growth corresponds to the constant critical energy release rate.

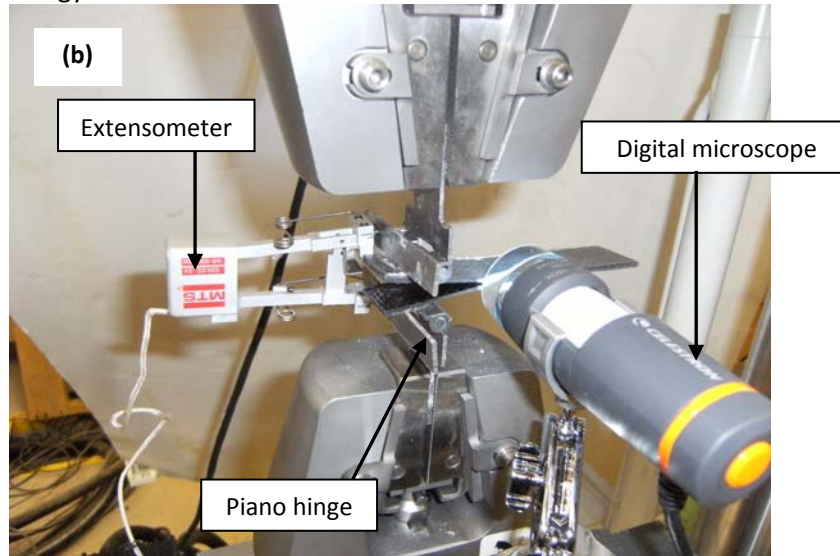


**Figure 18.** DCB test set-up for Interlaminar fracture toughness testing of CFRP incorporating MWCNTs.

It is important to report that the thickness of the composite slightly increases as the MWCNTs loadings increase. For instance, average thicknesses of 3.47, 3.58, 3.71, 3.80 mm were achieved with 0%, 0.5%, 1.0% and 1.5% MWCNT/epoxy FRP composites respectively. The increase in thickness approached 10% with the addition of 1.5% MWCNTs. Moreover, burn-off tests for the composite specimens were carried out according to ASTM D 3171. Fiber weight fractions of 60%, 58.8%, 56.25%, and 57.57% were observed for 0%, 0.5%, 1.0%, and 1.5% MWCNTs respectively. The slight increase in thickness and the decrease in fiber weight fraction with the addition of MWCNTs are attributed to the increase in the epoxy weight fraction and/or voids. It is well established that as the MWCNTs loading increases, the viscosity of the epoxy nanocomposite increases during the FRP fabrication. However, the slight change in thickness ( $\sim 10\%$ ) is expected to affect the stiffness of the specimens and have limited or no effect on the fracture toughness according to Eq. (1). Furthermore, since there is only one fracture plane for the DCB specimens, the slight increase in epoxy weight fraction is not expected to affect the fracture toughness of the composites either.

**Figure 19** shows sample microscopic images of the delamination growth and the corresponding load-displacement response for 0.5% MWCNTs epoxy FRP composites. The initial critical energy release rate

is calculated at the onset of delamination growth observed by microscope (point b). The subsequent energy release rates are calculated following the increase in delamination growth (points c-g). In addition, a comparison between the load-displacement curves of the FRP composites with various MWCNTs loadings is depicted in **Figure 19**. It is obvious from **Figure 19** that there is an increase in the peak load and its corresponding displacement with the addition of MWCNTs. Moreover, there is an apparent increase in the stiffness of composite specimens with the increase in MWCNTs loading due to the differences in thickness.

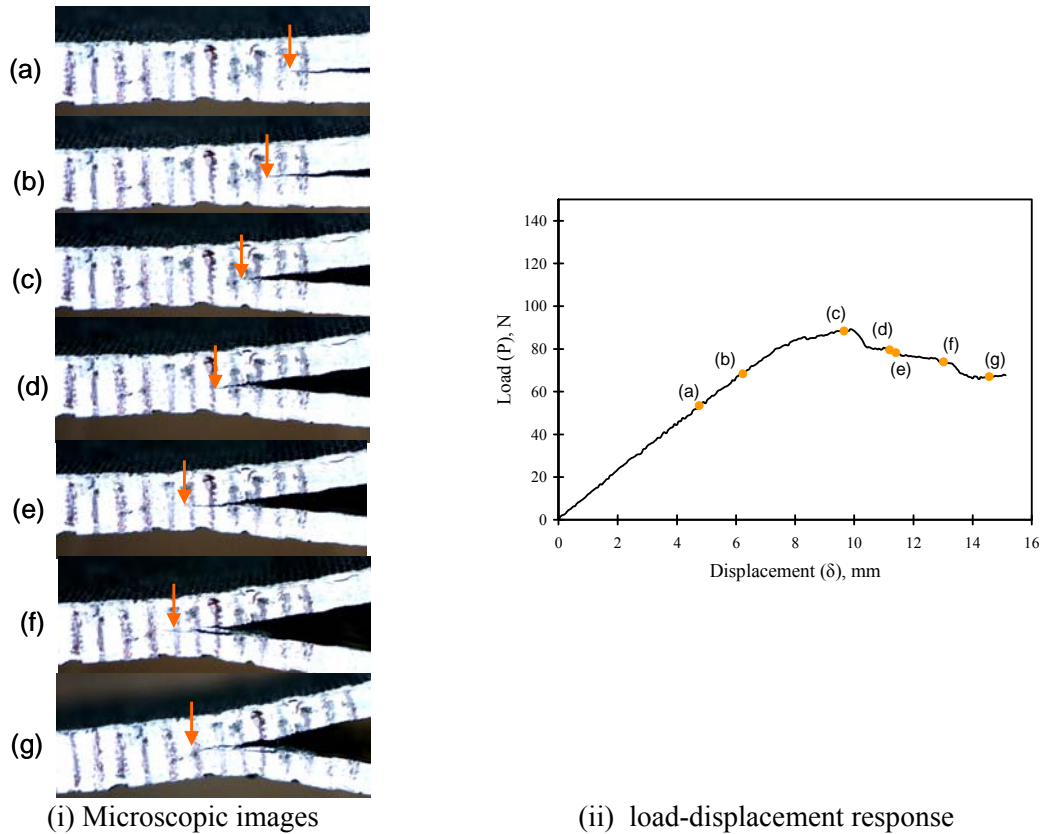


**Figure 19.** Crack propagation for the 0.5% COOH-MWCNT/epoxy FRP composites

The resistance curve (R-curve) shows the critical energy release rate  $G_{Ic}$  as a function of delamination length  $a$  as depicted in **Figure 20**. The data obtained for all the three specimens of each MWCNTs loading is predicted using third order polynomial fit. It is obvious that there is a significant effect of adding MWCNTs on the mode I critical energy release rate  $G_{Ic}$  of the FRP composites. As the MWCNTs loading increases, critical energy release rate increases. The highest enhancement in maximum critical energy release rate  $G_{Ic}$  approached 160% with the addition of 1.5% MWCNTs. The delamination growth mechanism is explained in **Figure 21**. In the neat epoxy FRP composites, the cohesive fracture of the matrix or the debonding between the fibers and the matrix resist the delamination growth at the crack tip. The addition of MWCNTs provides additional energy consumption mechanism due to the bridging effect of the MWCNTs at the interface. It is evident from the literature that fiber pull-out significantly increases the fracture energy release rate  $G_{Ic}$  of composites. It is believed that such mechanism exists here. The extremely high tensile strength of MWCNTs and the enhanced bond strength between the MWCNTs and the epoxy matrix would favor MWCNTs pull-out rather than rupture to be the dominant mechanism. Functionalization also plays an important role in enhancing the bond strength of the matrix

which allows MWCNTs pull-out to become an efficient energy consumption mechanism in the fracture process zone. Further studies at the microscale are needed to examine the delamination mechanism and its relation to MWCNTs length, diameter, and surface treatment.

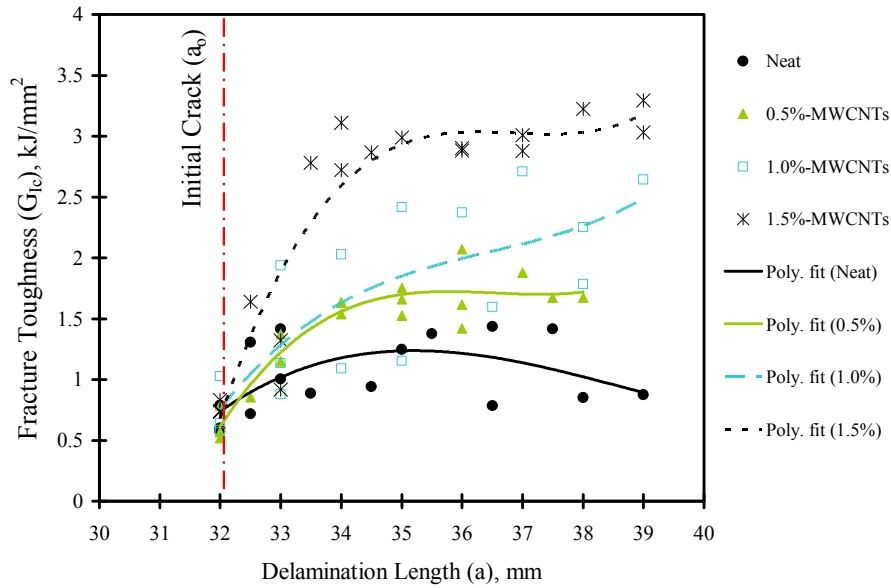


Figure 20. Resistance curve ( $R$ -curve) for MWCNT/epoxy FRP composites

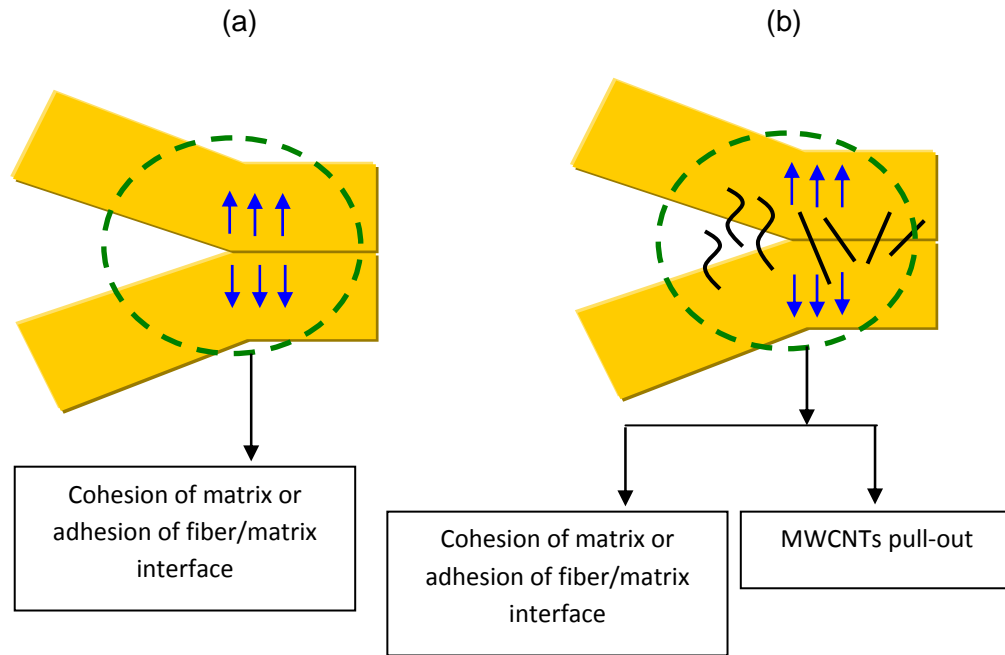


Figure 21. Schematic for delamination growth mechanism (a) neat epoxy FRP composites and (b) MWCNT/epoxy FRP composites

The initial and maximum critical energy release rates are compared in Figure 22. The figure shows that there is limited increase in the initial fracture energy release rate  $G_{Ic}$  while there is significant increase in the maximum fracture energy release rate  $G_{Ic}$  with the addition of MWCNTs. For example, the increase in the initial fracture energy release rate  $G_{Ic}$  approached 18% only with the addition of 1.5% MWCNTs, while the increase in the maximum fracture energy release rate  $G_{Ic}$  approached 160%. These

observations show that the effect of MWCNTs is limited at the beginning of the delamination growth and increases as the delamination length increases.

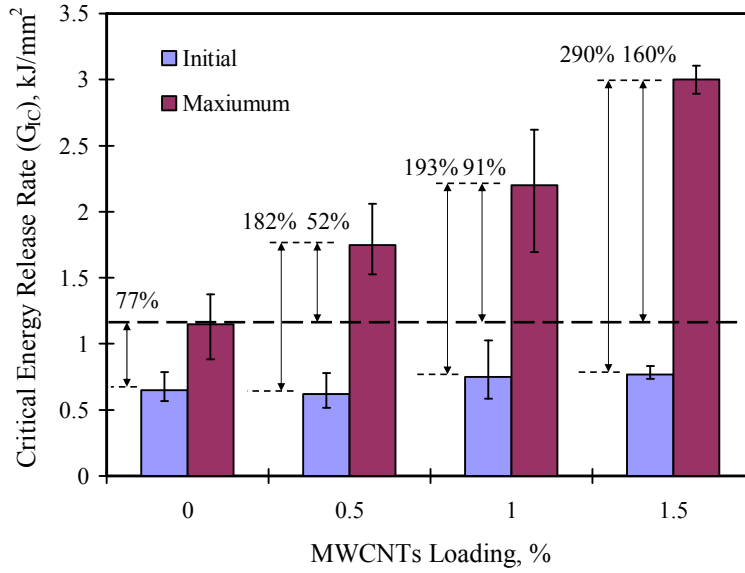


Figure 22. Comparison for the critical energy release rate corresponding to 6 mm delamination

### 3.10. Impact Testing

CEAST<sup>®</sup> 9350-Instron drop tower high velocity impact tester (Figure 23), recently acquired by UNM team, is used to conduct the transverse impact testing of the woven fabric composites. The test is performed by dropping a 12.7 mm diameter hemispherical striker carrying a total weight of 14.93 kg on the composite specimens from various heights and investigating the dynamic response. The total weight includes a carriage weight of 4.3 kg, a striker weight of 0.63 kg, and 10 kg additional weights. The sampling rate and the striker load capacity are 800 kHz and 21 kN respectively. In addition to the neat epoxy, three different COOH-MWCNTs loadings are examined; 0.5%, 1.0%, and 1.5% by wt. of epoxy. Five levels of energy are applied to the composites; 15, 24, 30, 60, and 120 J. The incident (initial) velocities for the five levels were 1.42, 1.8, 2.0, 2.85, and 4 m/sec and drop heights were 102.8, 165.2, 203.9, 414.1, and 815.7 mm respectively. The testing system is capable of measuring the time history for the force  $F(t)$  using the instrumented striker. The system is also equipped with a laser system to measure the incident velocity  $v_i$ . The following responses are then calculated in the time domain after ASTM D7136.

$$v(t) = v_i + gt - \int_0^t \frac{F(t)}{m} dt \quad (2)$$

$$\delta(t) = \delta_i + v_i t + \frac{gt^2}{2} - \int_0^t \left( \int_0^t \frac{F(t)}{m} dt \right) dt \quad (3)$$

$$E(t) = \frac{m[v_i^2 - v(t)^2]}{2} + mg\delta(t) \quad (4)$$

where  $t$  is time,  $m$  is the applied mass,  $\delta_i$  is the initial position,  $g$  is gravity,  $v(t)$  is the velocity,  $\delta(t)$  is the displacement, and  $E(t)$  is the absorbed energy.

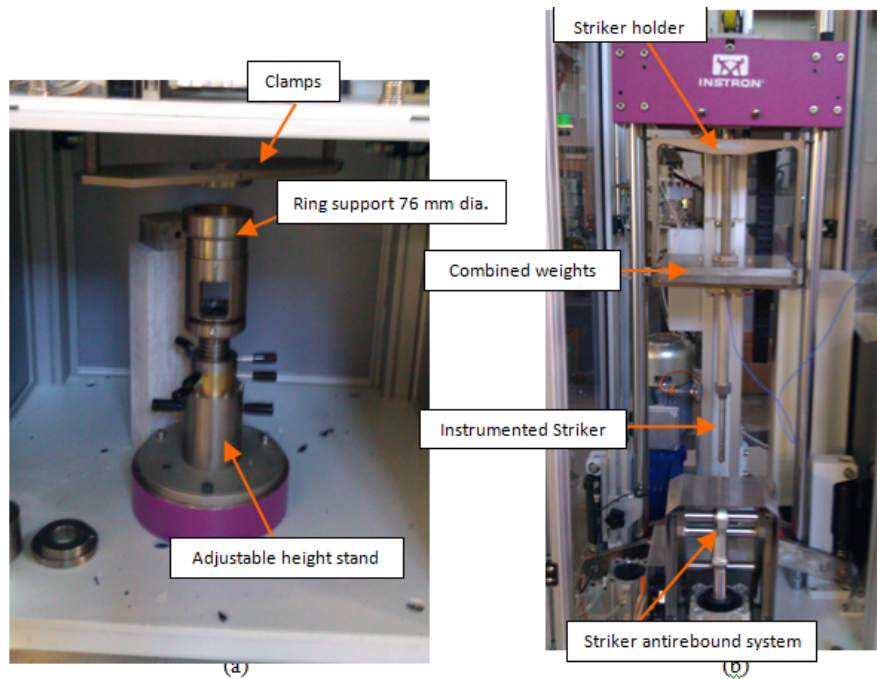


**Figure 23.** CEAST® 9350 impact tester (a) test chamber, and (b) turret.

**Figure 24** shows examples for the time history of the velocity during the impact test with different levels of applied energy. The positive values for the velocity represent downward motion for the striker while the negative values represent upward motion due to striker rebound. It can be noticed that the striker did not penetrate all composite specimens when energy of 15 J was applied [**Figure 24 (a)**]. Upon applying 24 J, the striker penetrated only the neat-epoxy composite plates while it rebounded from the composite plates reinforced by COOH-MWCNTs [**Figure 24 (b)**]. Moreover, the striker penetrated all composite specimens when energy of 30 J or above is applied [**Figure 24 (c)**]. The rate of change in velocity (deceleration) increases with the addition of nanotubes due to the increase in the stiffness of the composite plate. Below the penetration limit, the bounce point is defined as the point at which the striker's velocity approaches zero [see **Figure 24 (b)**]. In addition, the upward velocity is the final velocity at the end of the impact event after the rebound of the striker. The bounce time and upward velocity depend also on the stiffness of the tested specimens. It is observed that the addition of nanotubes decreased the bounce time and increased the upward velocity of the composite plates. For instance, Fig. 2 (d) shows a 25% decrease in bounce time with the addition of 1.5% COOH-MWCNTs. Furthermore, the bounce time increased by 20% as the applied energy increased from 15 to 24 J. This observation indicates that the nanotubes are capable of increasing the stiffness of the composite plates under impact loading.

An example of energy-time responses for various loadings of nanotubes is shown in **Figure 25 (a)** for the case of 30 J. The penetration (puncture) point, defined only above the penetration limit, is the point at which the force drops to 50% of the maximum or peak force according to the ISO standard. An average of 50 % improvement in penetration energy is observed by adding 1.0 or 1.5 % COOH-MWCNTs. The statistical analyses for the energy and other responses show that 50 % improvement in penetration energy is achieved by adding 1.0 or 1.5 % COOH-MWCNTs. The rate of energy absorption increases with the increase of the applied energy. Moreover, the penetration energy ( $E_p$ ), determined from the

energy levels above the penetration limit, does not depend on the applied energy since it is a material property.

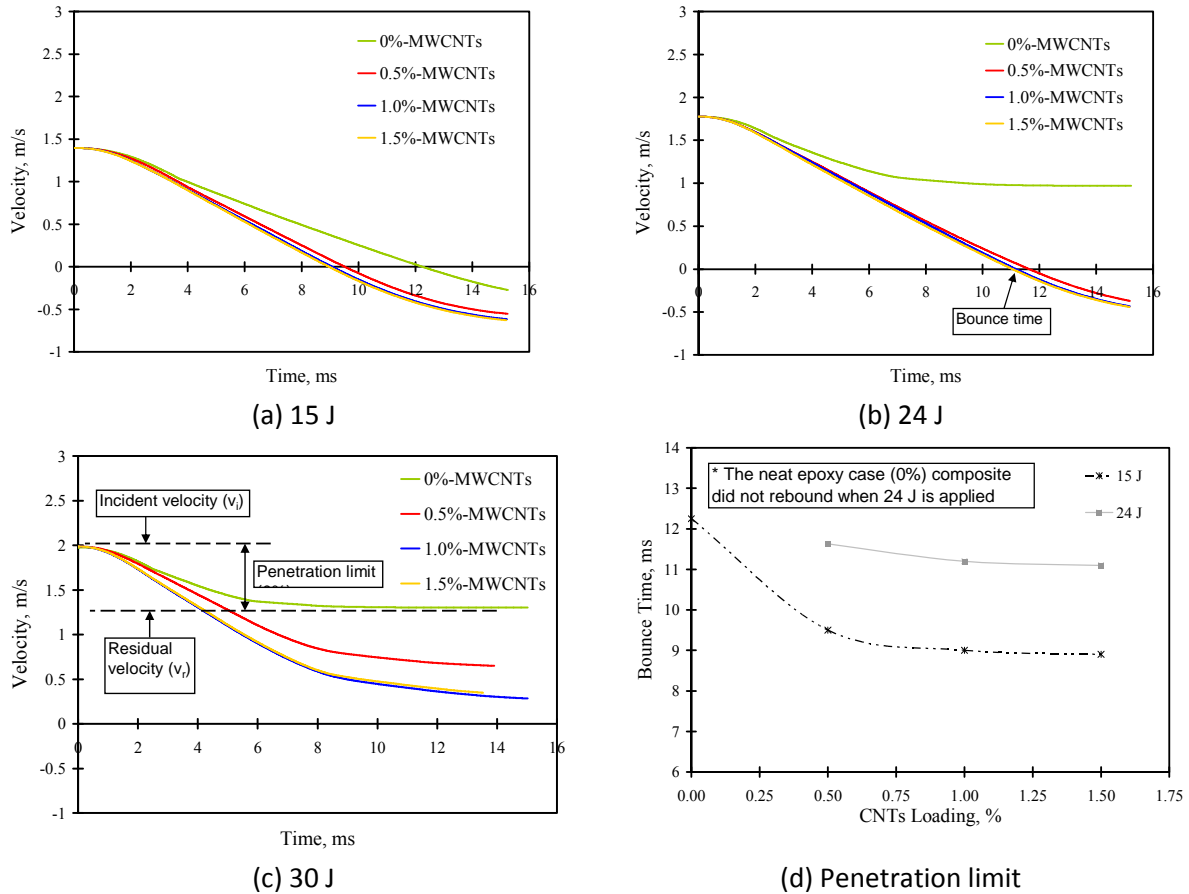


**Figure 24.** Velocity-time response for various COOH-MWCNTs composite plates subjected to different levels of energy (a) 15 J, (b) 24 J, (c) 30 J, (d) effect of CNTs loading on the bounce time.

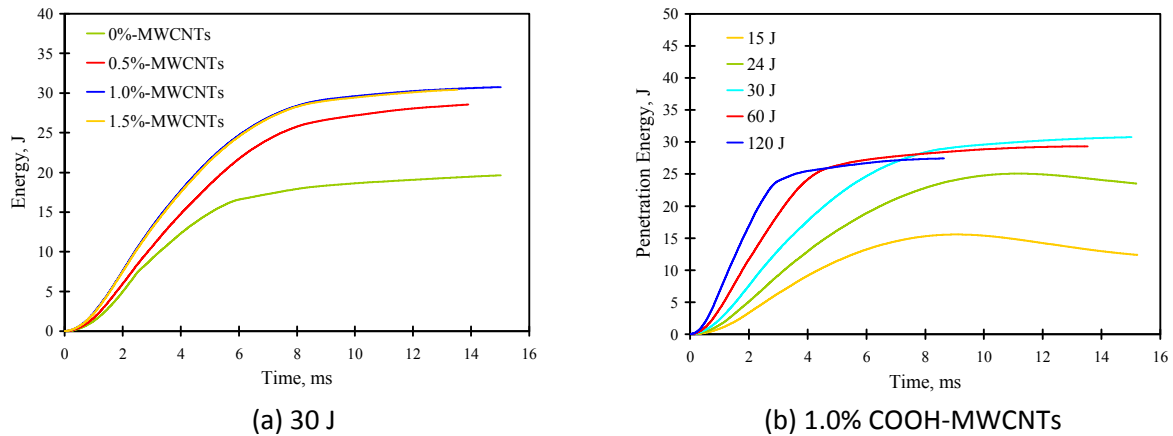


**Figure 25.** Energy-time response of COOH-MWCNTs FRP composite plates.

Examples of load-displacement responses for different COOH-MWCNTs loadings subjected to various levels of energy are shown in **Figure 26**. Based on statistical analysis using student t-test with 95% level

of confidence, no significant difference in peak force was observed between the different cases. This observation is attributed to the fact that fibers govern the load capacity of the composites. In addition, in the neat epoxy composite, the load drops abruptly upon reaching the maximum or peak force while in the COOH-MWCNTs epoxy composites the load remains constant to form a yield like plateau. Contradictory to most of the previous studies which used nano-materials to reinforce composites, the functionalized MWCNTs improved the impact response of the composite plates significantly.

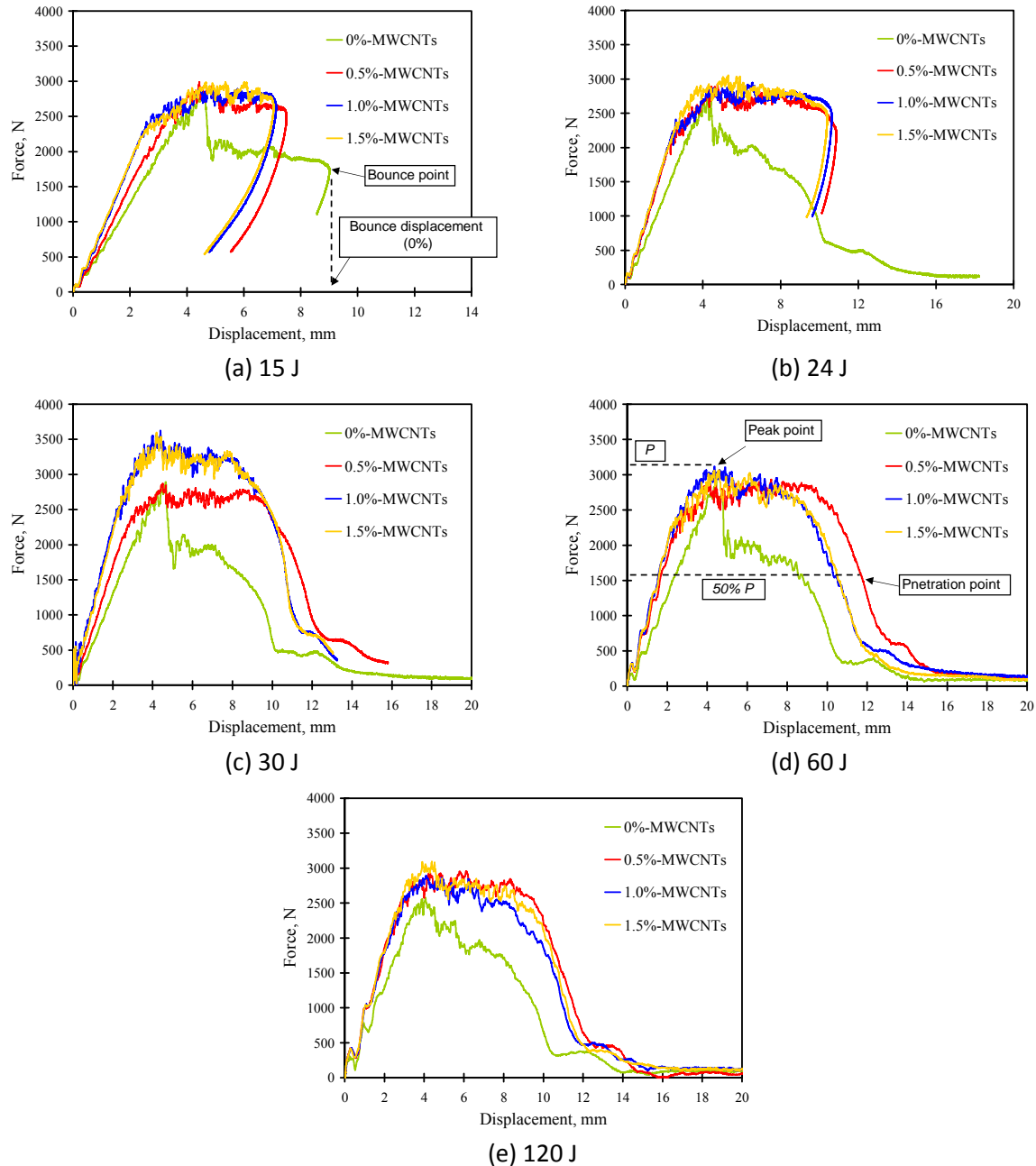


**Figure 26.** Load-displacement response for various COOH-MWCNTs composite plates subjected to different levels of energy.

**Figure 27** shows the four-sided pyramidal (tetrahedral) fracture is attributed to the bi-directional layout of the woven fabric composite plates. The fracture of the composite plates involves fiber and matrix

fractures. The damage size was evaluated by measuring the backplane damage of the pyramidal fracture. In particular, the damage height  $h_d$  and damage width  $w_d$ . Examples for the measurements of the damage deformations for different cases are shown in **Figure 27**.

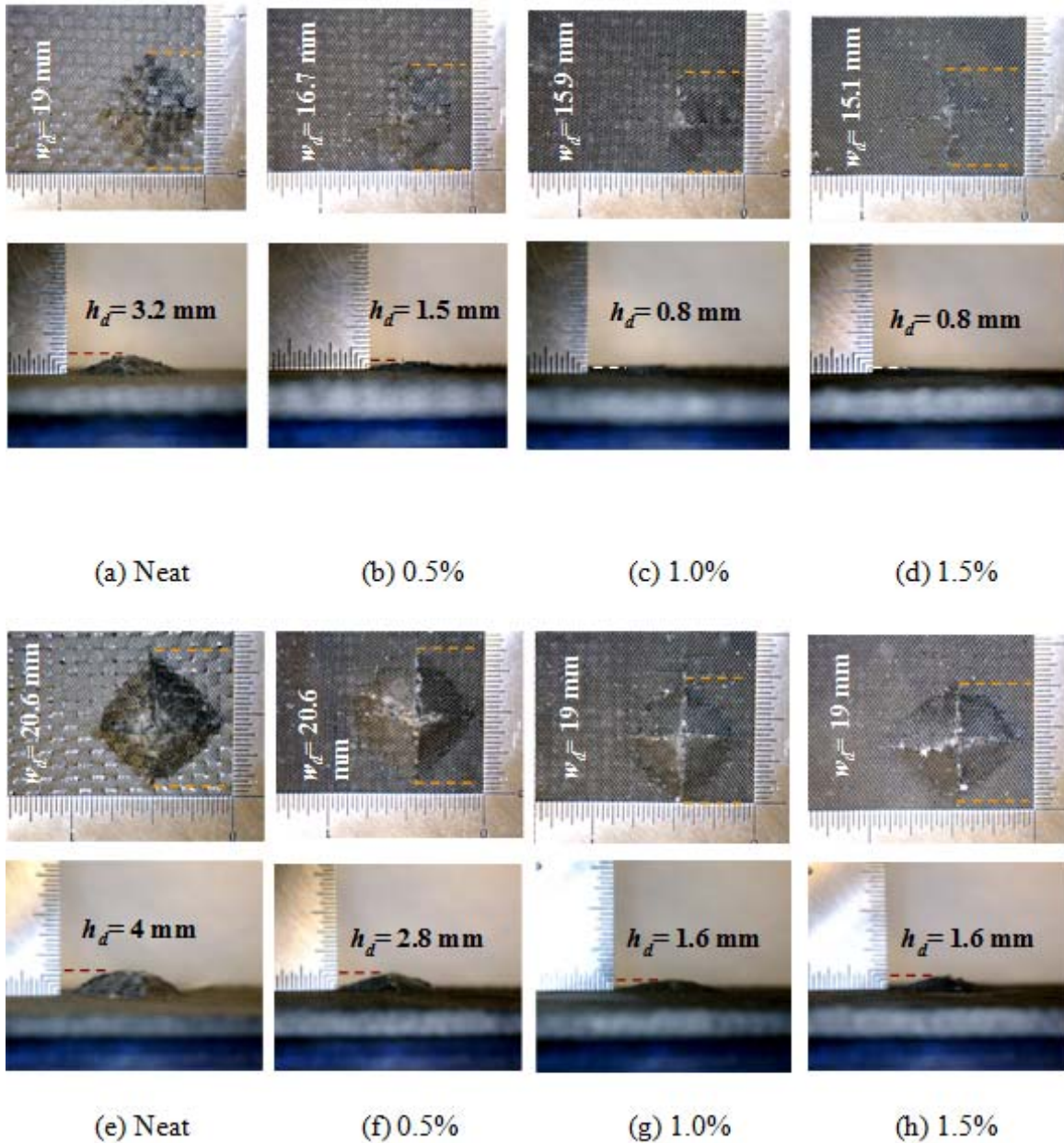


**Figure 27:** Damage of FRP composites subjected to various levels of energy (a-d) 15 and (e-h) 24 J

From **Figure 27**, it is observed that the carbon nanotubes have significant effect on damage size below the penetration limit. For instance, in the case of 15 J, the damage heights were 3.2, 1.5, 0.8, and 0.8 mm due to the addition of 0%, 0.5%, 1.0%, and 1.5% COOH-MWCNTs respectively. This yields 75% decrease in damage height with the addition of 1.5% COOH-MWCNTs. In addition, for the same applied energy, the damage widths were 19, 16.7, 15.9, and 15.1 mm due to the addition of 0%, 0.5%, 1.0%, and 1.5% COOH-MWCNTs respectively. A decrease of 20% in the damage width is observed with the addition

of 1.5% COOH-MWCNTs. Obviously; the nanotubes reduced the damage size significantly when composite plates are loaded below the penetration limit. On the other hand, the effect of nanotubes on the damage size is negligible above the penetration limit. Similar damage heights were observed with various nanotubes loadings when energy of 30 J or above is applied. However the damage width for the fracture of the composite plates above the penetration limit increased with the addition of nanotubes. For instance, the damage width associated with energy of 120 J were 20.6, 23, 22.2, and 22.2 mm due to the addition of 0%, 0.5%, 1.0%, and 1.5% COOH-MWCNTs respectively. This increase could be explained by the ability of the composites incorporating MWCNTs to absorb more energy (penetration energy) than the neat epoxy composites. The higher energy absorption causes more damage and therefore increases the damage width.

#### **4) Summary of Accomplishments**

In this study, the tensile behavior of the on-axis and off-axis MWCNTs composite coupons was examined. Significant improvements in the mechanical properties were observed in the off-axis tensile behavior of FRP incorporating functionalized MWCNTs. However, no significant effect of the MWCNTs was observed when the composite coupons were loaded on-axis. The pristine MWCNTs were shown to enhance the failure strain only while the functionalized MWCNTs were shown to enhance both the ultimate shear strength and failure strain. By incorporating 1.5% wt functionalized MWCNTs in the FRP composites, shear strength and strain improvements of 39 and 51% were achieved. These added improvements to the FRPs are due to the strong interfacial bond between the nanotubes and the epoxy matrix. Flexure and TGA tests of MWCNTs-epoxy nanocomposites confirmed that the strong interfacial bond between the functionalized MWCNTs and epoxy could improve the flexure strength and thermal stability of the nanocomposites. The reported improvement in the shear strength of the FRP composite can expand many applications of FRP composites governed by weak shear strength of the FRP.

Double lap joint tests for FRP composite substrates were performed to examine the performance of epoxy adhesive with carbon nanotubes. Three loadings of functionalized MWCNTs were examined and compared with the neat epoxy case; 0.5, 1.0, and 1.5% by wt. The experiments showed a significant nonlinearity in the stress-strain response of FRP lap splices incorporating CNTs. The use of MWCNTs results in enhancing the bond strength by 50% with 1.0% MWCNTs, Furthermore, enhancements in shear strain capacity and toughness reached about 700 and 1,100% respectively with 1.5% CNTs. The results suggest that CNTs can be used in shortening FRP lap splices or for enhancing energy absorption of FRP lap splices used in seismic retrofit of beam-column joints.

A significant effect of the MWCNTs on the interlaminar fracture toughness of composites. Limited effect is observed on the initial critical energy release rate (~18%) with the addition of 1.5% MWCNTs, however, a significant effect was observed on the maximum critical energy release rate (~160%). The increase in interlaminar fracture toughness might be attributed to the MWCNTs' bridging effect. A considerable nonlinearity of the R-curve was observed with a significant increase in the initial critical energy release rate which suggests that LEFM might not be the most suitable method of analysis to explain fracture of epoxy incorporating MWCNTs.

Experimental investigation of low-velocity impact strength of transverse woven carbon fabric composites is conducted with various loadings of functionalized multi-walled carbon nanotubes (0%, 0.5%, 1.0%, and 1.5% by wt. of epoxy). The composite plates were subjected to five different levels of energy; 15, 24, 30, 60, and 120 J. The experiments showed that below penetration limit, same peak force and 50% improvement in penetration energy are observed using 1.5% COOH-MWCNTs by weight

of epoxy. Above the penetration limit, the penetration energy remains the same regardless of the applied energy while the penetration limit decreases as the applied energy increases. It is also observed that increasing the MWCNTs content can significantly limit the damage size only below the penetration limit. In general, the use of functionalized MWCNTs significantly improved the low-velocity impact response of the transverse woven composite plates under impact

## **5) Personnel supported**

### Faculty

- 1- Mahmoud Reda Taha (PI, UNM, Civil Engineering)
- 2- Marwan Al-Haik (Virginia Tech, Mechanical Engineering)
- 3- Claudi Luhrs (Co-PI, UNM, Mechanical Engineering)
- 4- Hamid Garmestani (Georgia Tech, Mechanical and Materials Engineering)

### Post Doctors

- 1- Jung Joong Kim (Post-doc, UNM, Civil Engineering)

### Students Graduated Under This Project

- 1- Michael Sheyka (PhD– UNM, Mechanical Engineering, 2011)
- 2- Eslam Soliman (PhD – UNM, Civil Engineering, 2011)
- 3- Sherif Abobakr (MS– UNM, Civil Engineering, 2012)
- 4- Dan Garcia (MS- UNM, Mechanical Engineering, 2010)
- 5- Hoda Amani (PhD, Georgia Tech, Mechanical and Materials Engineering)
- 6- Mehran Tehrani (PhD – Virginia Tech, Mechanical Engineering, 2012)

## **6) Scholarly Journal Publications**

1. International Journal of Material & Structural Integrity, Special Issue on Nanotechnology for Structural Materials. Guest Editors: Reda Taha, M.M. and Al-Haik, M., Vol. 3, No. 2/3, 2009, pp. 99-260.
2. Al-Haik, M., Dai, J., Garcia, D., Chavez, J., Reda Taha, M.M., Luhrs, C. and Phillips, J. "Novel Growth of Multiscale Carbon Nanofilaments on Carbon and Glass Fibers", *Journal of Nanoscience & Nanotechnology Letters*, Vol. 1, No. 2, 2009, pp. 121-127.
3. Luhrs, C., Garcia, D., Tehrani, M., Al-Haik, M., Reda Taha, M.M. and Philips, J. "Generation of Carbon nanofilaments on Carbon Fibers at 550 oC", *Carbon*, Vol. 47, No. 13, 2009, pp. 3071-3078.
4. Reda Taha, M.M., Colak-Altunc, A.B. and Al-Haik, M. "A Multi-Objective Optimization Approach for Design of Blast Resistant Carbon Fiber-Epoxy Composite Laminates Using Carbon Nanotubes", *Journal of Composite B: Engineering*, Vol. 40, No. 6, 2009, pp. 522-529.
5. Reda Taha, M.M., Masia, M.J., Choi, K-K., Shrive, P.L. and Shrive, N.G. "Creep Effects in Plain and FRP-Strengthened RC Beams", *ACI Structural Journal*, Vol. 107, No. 6, pp. 627-635, 2010.
6. Li, D. S., Baniassadi, M. Garmestani, H. Ahzi, S., Reda Taha, M.M. and Rush, D. "3D Microstructure Reconstruction of Carbon Nanotube Composites Using Correlation Function", *Journal of Computational and Theoretical Nanoscience*, Vol. 7, 2010, pp. 1462-1468.
7. Al-Haik, C., Reda Taha, M. M., Luhrs, M.M., Roy, A., Dai, L., Phillips, J. and Doorn, S. "Hybrid Carbon Fibers/Carbon Nanotubes Structures for Next Generation Polymeric Composites", *Journal of Nanotechnology*, Vol. 2010, Article ID 860178, 2010, 9 pp., doi:10.1155/2010/860178.

8. Al-Haik, M., Leseman, Z, Luhrs, C. Reda Taha, M.M., "Introducing Nanotechnology to Mechanical and Civil Engineering Students through Materials Science Courses", *Journal of Nano Education*, Vol. 2, pp.1-14, doi:10.1166/jne.2011.1008, 2011.
9. Altunc, A. B., Kim, J. J., Al-Haik, M., Reda Taha, M.M. "Reliability-based Design of Blast Resistant Composite Laminates Using Carbon Nanotubes", *Composite Structures*, Vol. 93, pp: 2042-2048, 2011.
10. Soliman, E., Kandil, U. and Reda Taha, M.M. "Limiting Shear Creep of Epoxy Adhesive at the FRP-Concrete Interface Using Multi-Walled Carbon Nanotubes", *International Journal of Adhesion and Adhesives*, Vol. 33, pp: 36-44, 2012.
11. Soliman, E., Kandil, U. F., Reda Taha, M.M. "The Significance of Carbon Nanotubes on Styrene Butadiene Rubber (SBR) and SBR Modified Mortar", *Materials and Structures*, Vol. 45, No. 6, pp. 803-816. 2012.
12. Soliman, E., Sheyka, M. and Reda Taha, M.M. "Low Velocity Impact of Thin Woven Carbon Fabric Composites Incorporating Multi-Walled Carbon Nanotubes", *International Journal of Impact Engineering*, Vol. 47, pp. 39-47, 2012.
13. Sheyka, M., Altunc, A. B., and Reda Taha, M.M. "Multi-Objective Genetic Topological Optimization for Design of Blast Resistant Composites", *Applied Composite Materials*, In press, 2012.
14. Soliman, E., Al-Haik, M., Reda Taha, M.M. "On and off-axis tension behavior of fiber reinforced polymer (FRP) composites incorporating multi-walled carbon nanotubes", *Journal of Composite Materials*, In press, 2012.
15. Soliman, E., Kandil, U. and Reda Taha, M. M. "Enhancing Interlaminar Fracture toughness of Woven FRP Composite Using Carbon Nanotubes", *Journal of Composites B: Engineering* submitted January 2012, In Review.

**7) Papers in Conference Proceedings and Public Presentations**

1. Sheyka, M., Colak-Altunc, B., Reda Taha, M. M., Cruz, G., Connolly, T., Tortorelli, D. "Multi-objective Blast Resistant Composite Plate Design Optimization" *51st AIAA Conference*, Orlando, FL. April 2010.
2. Dai, J., Soliman, E., Safdari, M., Al-Haik, M., Reda Taha, M. M., "Effect of Carbon Nanotube Growth Conditions on Strength and Stiffness of Carbon and Glass Fiber Polymer Composites", *51st AIAA Conference*, Orlando, FL. April 2010.
3. Colak-Altunc, B., Kim, J. J., Al-Haik, M., Reda Taha, M. M. "Probabilistic Design of Blast Resistant Composites Using Carbon Nanotubes", *51st AIAA Conference*, Orlando, FL. April 2010.
4. Soliman, E., Kandil, U.F., Reda Taha, M.M., "Creep of Fiber Reinforced Polymer-Epoxy-Concrete Interface Incorporating Carbon Nanotubes", *Proceedings of the First Middle East Conference on Smart Monitoring, Assessment and Rehabilitation of Civil Structures, SMAR 2011*, Dubai, UAE, February 2011
5. Sheyka, M. P., Kim, J-J., Altunc, A. B., and Reda Taha, M. M. "A Reliability-based Energy Approach for Design Optimization of Blast Resistant Composites", *Proceedings of the ASME International Mechanical Engineering Conference & Exposition, IMECE. Denver, CO. USA*, November 2011
6. Soliman, E., Kandil, U. F. and Reda Taha, M. M. "Carbon Nanotubes for Shortening FRP Lap Splice", *Proceedings of 6th International Conference on Advanced Composite Materials in Bridges and Structures (ACMBS)*, Kingston, Ontario, Canada, May 2012.

**8) New discoveries, inventions, or patent disclosures.(If none, report none)**

1. Method for Making Multi-Scale Carbon-Carbon Structures for Use in Composites. (UNM-0895) Al-Haik, M., Luhrs, C., Philips, J. and Reda Taha, M.M., *Patent Filed, November 2009.*
2. Hybrid Carbon Fiber Carbon Nano Tube Structures based on Different Iron Catalysts Deposition Methods (UNM-0929). Al-Haik. M., Luhrs, C., Philips, J. and Reda Taha, M.M., *Patent Filed, November 2009.*
3. A New Latex Modified Concrete Incorporating Carbon Nanotubes, (UNM-1033) Reda Taha, M.M., Kandil, U. and Soliman, E. Patent Filed, May 2011

**9) Honors/Awards - list honors, degrees, and awards received during the grant period**

1. M. Sheyka and E. Soliman, PhD with Distinction, UNM School of Engineering, December 2011.
2. Dr. Mahmoud Reda Taha, UNM School of Engineering, Junior Faculty Research Excellence Award, University of New Mexico, May 2010.
3. Dr. Mahmoud Reda Taha, ACI Walter Moore Jr. Faculty Achievement Award, American Concrete Institute, March 2010.
4. Dr. Mahmoud Reda Taha Army Office of Research Award: DURIP: High Velocity Impact Equipment, May 2010.
5. Dr Marwan Al-Haik and Dr. Mahmoud Reda Taha, Army Office of Research Award: DURIP: Instrumentation for Nanoscale Enhanced Impact Resistance for Optimized Structures, May 2009.
6. Jeremy Chavez. Honor Undergraduate Thesis, Growth of carbon nanotubes/nanofibers on the surface of carbon fibers. Advisor Marwan Al-Haik May 2009, Department of Mechanical Engineering UNM.

**10) Quad chart.**



**Next Generation Structural Composites Using Surface Grown Carbon Nanotubes, PI: Mahmoud Reda Taha, University of New Mexico, HDTRA1-08-1-0017**

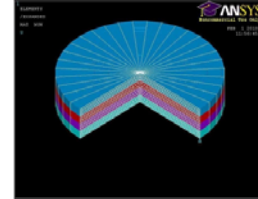
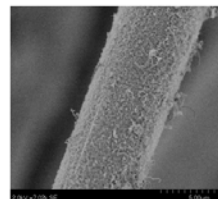
To Produce and characterize the next generation composites with enhanced blast resistance. The new composite will be developed by growing carbon nanotubes (CNT) on surface of carbon fibers – using our novel technique graphitic structures by design (GSD) - prior to impregnate the fibers in polymer/cement matrix.

**Challenges:**

- Grow carbon nanotubes at low temperatures
- Disperse CNT-carbon fibers in polymers and cements.
- Perform a comprehensive multi-scale characterization program in relevance to blast resistance
- Examine the impact strength of the new composite

**Benefits of Proposed Effort:** Bringing the proposed investigations to fruition will pave the road for creating the next generation composite materials with ultra high strength, fracture toughness and deformability that is capable of mitigating blast events much more efficiently than current composite technology.

**Personnel Support:** Five faculty members from two institutions (University of New Mexico (PI) and Georgia Institute of Technology (Co-PI) will be working on the project. Two Post-doctors and Six PhD, MSc and undergraduate students are supported by this research effort.



Work on progress by the PIs showing SEM image of surface grown CNT on carbon fibers and simulation for CNT carbon fiber laminates (*non published work*)

**Bullet list of the major goals/milestones by Project year**  
 Year1 – Grow CNT & nano- characterization  
 Year 2 – Create composites & micro -characterization  
 Year 3 – Macro- characterization & Impact testing

**Funding Profile**

Year 1 Dates	Year 2 Dates	Year 3 Dates
429,214	360,929	333,666
11/15/07-11/14/08	11/15/08 – 11/14/09	11/15/09–11/14/10

**PI Contact Information**

Mahmoud Reda Taha, [mrtaha@unm.edu](mailto:mrtaha@unm.edu),  
 Phone: 505-277-1258 Fax: 505-277-1988

**DISTRIBUTION LIST  
DTRA-TR-12-46**

**DEPARTMENT OF DEFENSE**

DEFENSE TECHNICAL  
INFORMATION CENTER  
8725 JOHN J. KINGMAN ROAD,  
SUITE 0944  
FT. BELVOIR, VA 22060-6201  
ATTN: DTIC/OCA

DEFENSE THREAT REDUCTION  
AGENCY  
8725 JOHN J. KINGMAN ROAD,  
STOP 6201  
FT. BELVOIR, VA 22060-6201  
ATTN: J. REED

**DEPARTMENT OF DEFENSE  
CONTRACTORS**

EXELIS, INC.  
1680 TEXAS STREET, SE  
KIRTLAND AFB, NM 87117-5669  
ATTN: DTRIAC